

DATE ISSUED MAR 10 1979

ORNL/TM-6662

781101

ORNL
REPRODUCED COPY

Conceptual Study for a Laser Disassembly Development Unit

J. P. Carstens
B. S. Weil

OAK RIDGE NATIONAL LABORATORY
OPERATED BY UNION CARBIDE CORPORATION - FOR THE DEPARTMENT OF ENERGY

ORNL/TM-6662
Dist. Category UC-79c

Contract No. W-7405-eng-26

03

CONSOLIDATED FUEL REPROCESSING PROGRAM

CONCEPTUAL STUDY FOR A LASER DISASSEMBLY DEVELOPMENT UNIT*

J. P. Carstens
United Technologies Research Center

B. S. Weil
Chemical Technology Division 03

Date Published: February 1979

NOTICE: This document contains information of a preliminary nature. It is subject to revision or correction and therefore does not represent a final report.

*Extracted from a final report on work under Subcontract 73X-56956V.

Prepared by the
OAK RIDGE NATIONAL LABORATORY
Oak Ridge, Tennessee 37830
operated by
UNION CARBIDE CORPORATION
for the
DEPARTMENT OF ENERGY

CONTENTS

	<u>Page</u>
LIST OF FIGURES	v
ABSTRACT	1
1. SUMMARY	1
2. INTRODUCTION	2
3. SCOPE OF STUDY	5
4. LASER CUTTING TESTS	6
4.1 Objective	6
4.2 Laser Test Equipment	6
4.3 Procedure	6
4.4 Test Variables	7
4.4.1 Power and speed	7
4.4.2 Gas jet-assist	8
4.4.3 F/number	8
4.4.4 Angle of incidence	8
4.4.5 Beam mode	9
4.4.6 Purge	10
4.5 Test Results and Discussion	10
4.5.1 Initial testing	12
4.5.2 Power and speed test	14
4.5.3 Gas jet-assist	15
4.5.4 Focal length test	19
4.5.5 Incident angle tests	19
4.5.6 Corner removal test	21
4.5.7 Argon purge test	21
4.5.8 Dummy rod test	23
5. LASER-CUTTING SYSTEM ANALYSES	25
5.1 Focus Head Control Schemes	25
5.1.1 Full length data storage	25
5.1.2 Partial length data storage	26
5.1.3 Open-loop control	26
5.1.4 Closed-loop control	26
5.1.5 Mechanical control	27
5.2 Shroud Surface Sensors	27
5.2.1 Optical sensor	28
5.2.2 Capacitive or inductive sensors	29
5.2.3 Mechanical sensor (rollers)	30
5.2.4 Fluidic sensors	30
5.3 Selected Focus Head Control and Sensor Systems	31
5.4 Optical Components	34
5.4.1 Laser optics in the hot cell	34
5.4.2 Laser window	38
5.5 Laser Heat and Mass Contributions to the Hot Cell	40

6.	SYSTEM DESIGN	42
6.1	Laser-Cutting System Description	42
6.1.1	Gantry assembly	44
6.1.2	Focus head assembly	45
6.1.3	Shroud follower assembly	49
6.1.4	Calibration station	53
6.1.5	Typical cutting sequence	53
6.1.6	System features to be designed	54
6.2	System Specification	54
6.2.1	Laser system and optical train	55
6.2.2	Focus head features	55
6.2.3	Mechanical	56
7.	CONCLUSIONS	56
8.	RECOMMENDATIONS	58
	REFERENCES	59

LIST OF FIGURES

<u>Figure</u>		<u>Page</u>
2.1	Dimensions of CRBR core fuel subassembly.	2
3.1	Laser cutting scenario.	5
4.1	Laser cutting process variables.	7
4.2	Cutting test configurations.	9
4.3	Laser cutting focusing optics.	10
4.4	Results of plate-on-plate laser cut.	12
4.5	Laser cutting fixture.	13
4.6	Laser cut specimens cut at 1.5 kW and 50 cpm.	14
4.7	Jet-assist configurations.	16
4.8	Comparison of laser cuts made with varying amounts of oxygen in jet assist.	17
4.9	Laser cut using CO ₂ jet assist.	18
4.10	Laser cut using He jet assist.	19
4.11	Specimens cut with the laser beam oriented at 45° to the plate surface.	20
4.12	Laser cut specimens with argon gas between the fuel pin and shroud wall.	22
4.13	Laser cut specimens with solid dummy rods underneath shroud.	24
5.1	Optical sensor technique.	28
5.2	Capacitive or inductive sensor technique.	29
5.3	Direct drive fluid sensor technique.	31
5.4	Fluid sensor boost arrangement.	33
5.5	Maximum transfer mirror temperature during beam on-time.	37
6.1	The laser cutting system.	43
6.2	Isometric view of laser cutting system.	44

<u>Figure</u>		<u>Page</u>
6.3	Focus head assembly.	46
6.4	Isometric view of focus head assembly.	47
6.5	Circumferential shroud follower.	50
6.6	Longitudinal shroud follower.	51
6.7	Exploded view of shroud follower assembly.	51

CONCEPTUAL STUDY FOR A LASER DISASSEMBLY DEVELOPMENT UNIT*

J. P. Carstens and B. S. Weil

ABSTRACT

Several inherent characteristics of laser cutting suggest the desirability of the usage of this technique to cut metal in a hot cell. The study results indicate the basic feasibility of laser cutting for the disassembly of fast reactor fuel subassemblies. Presented in this report are the results of tests performed, a systems analysis, and a conceptual design for a developmental disassembly laser unit.

1. SUMMARY

The study results indicate the basic feasibility of laser cutting for the disassembly of fast reactor fuel subassemblies. The study involved laser cutting tests, analyses of tooling systems and optical components, and the conceptual design of a disassembly unit.

Tests were run at the 1.5 to 10 kW power level using continuous wave CO₂ electric discharge lasers in the industrial laser test laboratory at United Technologies Research Center (UTRC), East Hartford, Connecticut. Laser cuts were made into specimens of shroud backed up by empty fuel rods with and without 1.5-mm spacer wire wrapping. Laser power, speed, gas-assist jet location, gas jet size, gas composition, laser beam mode, and system focal length were among the parameters varied in the course of the test work.

Consideration was given to alternate focus head schemes and different guidance arrangements to sense the location of the fuel subassembly shroud. Optical components for applications in the hot cell were evaluated, and a mirror distortion analysis was performed to ascertain the feasibility of using uncooled copper mirrors. Attention was given to the "windows" through which the unfocused laser beam could be directed into the hot cell. Also considered was the effect of laser cutting on the cell heat load and mass balance.

* Extracted from a final report on work under Subcontract 73X-56956V.

2. INTRODUCTION

Oak Ridge National Laboratory (ORNL) is developing equipment and processes to recycle fuel from fast breeder reactors and other nuclear fuel cycles. Reprocessing the fissionable material contained in irradiated subassemblies includes, as initial steps, removing the outer shroud from the fuel rods and shearing the fuel rods as a bundle into short lengths. This facilitates chemical leaching of the fissionable material from the remaining metallic waste.

A typical fast breeder reactor fuel subassembly consists of 6-mm-diam fuel rods containing the fissionable material. Each rod is wrapped with 1.5-mm-diam spacer wire, arranged into a 217-rod bundle, and enclosed in a 3-mm-thick hexagonal shroud, as shown in Fig. 2.1.

For some time, work has been under way in Great Britain and France to develop laser-cutting concepts for nuclear fuel disassembly. In

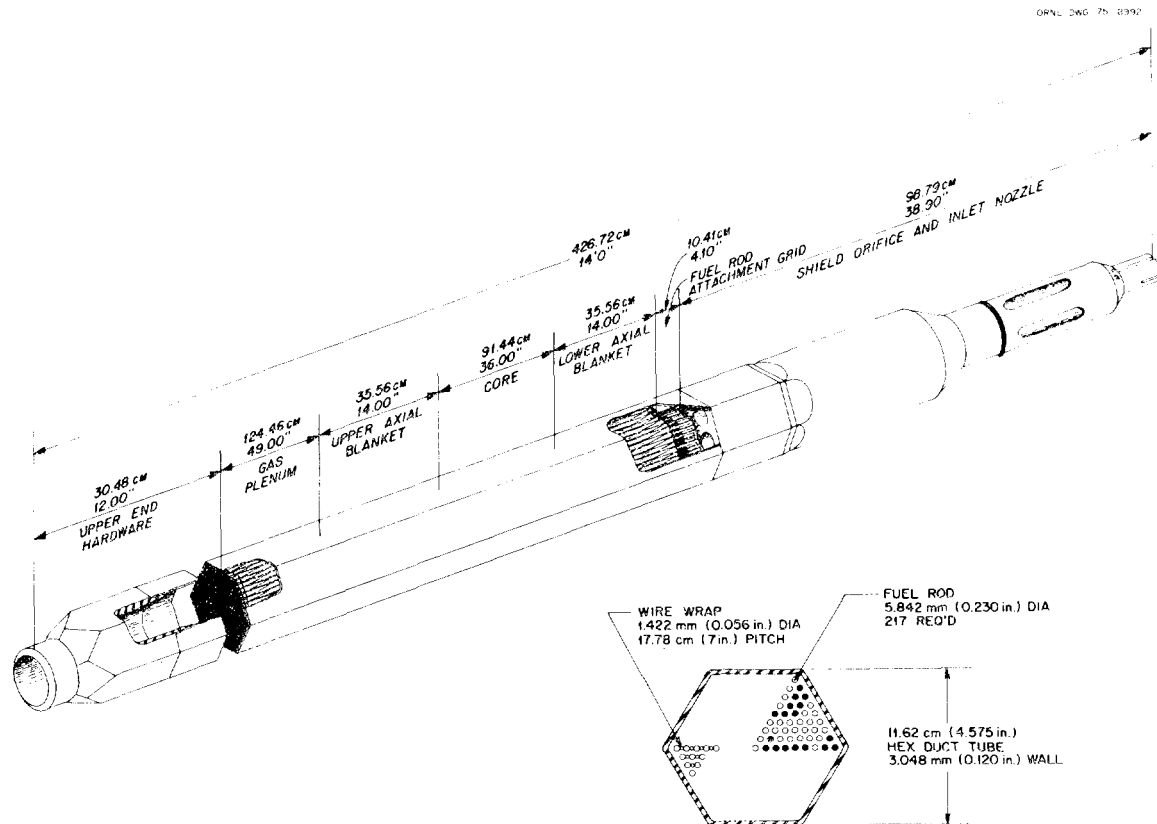


Fig. 2.1. Dimensions of CRBR core fuel subassembly.

Britain, development has resulted in two 400-W laser systems that remove upper and lower end hardware, open canisters, and also remove sections of shroud prior to complete disassembly.¹⁻³ Both of these systems are expected to be in full operation, processing the prototype fast reactor fuel, by the spring of 1979. A report from France outlines the results of test cuts at the 250- to 750-W power level and presents a preliminary system concept for a laser-cutting system in a hot cell.⁴ These few references indicate that laser cutting of nuclear fuel subassemblies is under careful examination in Europe.

Although some previous work has considered the use of pulsed and low-powered CO₂ lasers for cutting and welding nuclear fuel rods during postirradiation examination,^{5,6} this report is the first systematic consideration of high-power cw CO₂ laser cutting of fast breeder reactor fuel subassemblies performed in the United States.

The following environmental problems and system design criteria were established by ORNL to evaluate any cutting technique for removing the outer shroud prior to shearing.^{7,8}

1. The amount of dross, or cut material lost to the general environment of the hot cell, should be minimized.
2. The amount of fissionable fuel (contained inside the fuel rods), vaporized or otherwise lost to the hot-cell environment, should be minimized.
3. The cutting system must be capable of reliable remote operation and maintenance while performing in a gamma-radiation environment of 5×10^6 rd/h with possible fuel subassembly temperatures in the range of 260 to 520°C (ambient temperature in the hot cell is 20 to 40°C).
4. The expendables required by the cutting system, including degradable components, gases, and fluids, should be minimized so as not to add significantly to the decontamination and waste conditions already inherent in the disassembly operation.
5. The cutting system should be of a modularized design to facilitate remote removal and replacement of any portion of the system.

Several inherent characteristics of laser cutting suggest the desirability of the usage of this process to cut metal in a hot cell. These are:

1. No force is exerted on the subassembly by the cutting process itself.
2. Compared to other metal removal techniques, the amount of material vaporized or lost as slag from the cut region is minimal, due to the characteristically small kerf of laser cutting.
3. The laser cutting process can be readily automated by suitable indexing of the beam transfer and focusing mirrors.
4. The laser itself can be located outside the hot cell, which greatly reduces the complexity of the laser cutting system in the hot cell.
5. In-cell system components can be relatively small, easy to maintain, and tolerant of the radioactive and corrosive environment in the hot cell.

Determination of the extent to which these inherent advantages can be achieved in an actual laser cutting system is the major goal of the work reported here.

3. SCOPE

The purpose of the work reported herein is to evaluate the merits of the laser for the cutting of reactor fuel subassembly shroud. This involves making a circumferential cut at one end of the subassembly, a longitudinal cut to the other end of the subassembly, and then a second circumferential cut. The approximate locations of these cuts into the 3-mm-thick, type 316, 20% cold-work stainless steel shroud are shown in Fig. 3.1.

ORNL DWG. 77-4783

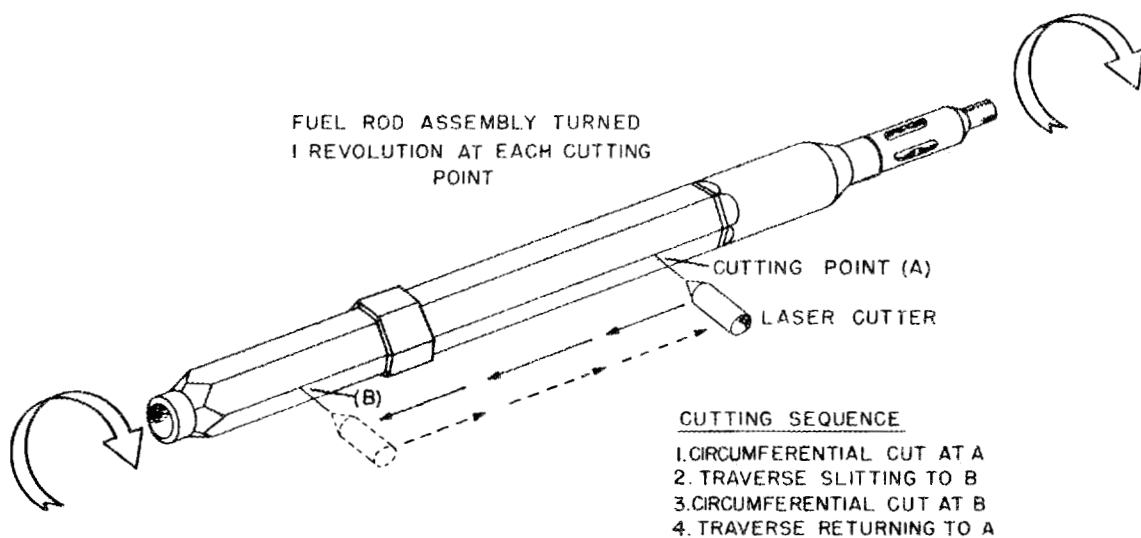


Fig. 3.1. Laser cutting scenario.

4. LASER CUTTING TESTS

4.1 Objective

As shown in Fig. 2.1, the hexagonal shroud is made of 3-mm-thick stainless steel. For spacing when packed into the shroud, the fuel rods are wrapped with 1.5-mm-diam wire using a 10-cm pitch. However, warpage of the rods during irradiation in the reactor can force the rods into direct contact with the shroud in random regions.

Laser cutting tests were conducted to determine the feasibility of cutting a nuclear fuel subassembly shroud without puncturing the cladding of the interior oxide bearing fuel rods.

4.2 Laser Test Equipment

The laser cutting experiments described in this report were conducted on two multikilowatt CO₂ lasers located at the UTRC facility. The majority of the cutting was performed on a laser equipped with unstable resonator optics. This produces an output beam with an intensity distribution in the shape of an annulus (no laser power over an inner diameter of the laser beam). The remainder of the work was conducted using a laser whose beam intensity distribution is gaussian (i.e., peaked at the beam centerline).

4.3 Procedure

Laser cutting tests were conducted by cutting through 3-mm-thick simulated shroud sections of type 304 stainless steel with 6-mm-diam, 0.4-mm wall tubes located directly under the beam impingement point. The tubes were located in either direct surface contact with the plate material or spaced away from the plate by wire. Some cutting tests were also performed to demonstrate a dummy fuel pin concept by using a solid rod under the stainless steel plate.

4.4 Laser Test Variables

The laser cutting process variables evaluated as part of this program are listed and are illustrated in Fig. 4.1. Optimum values of these variables are not independent, but have a strong dependence on one another.

ORNL DWG. 78-19439

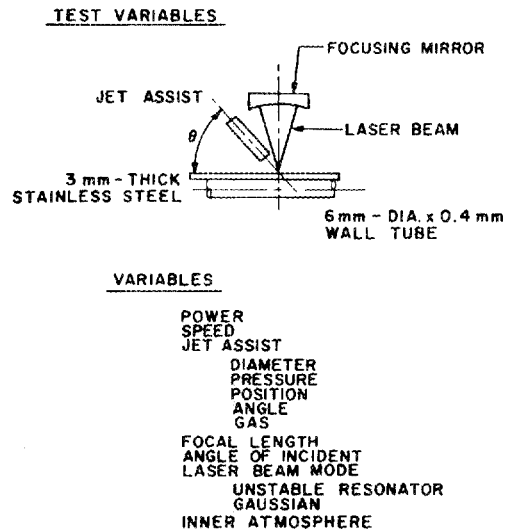


Fig. 4.1. Laser cutting process variables.

4.4.1 Power and speed

Laser power and speed are closely related, especially under conditions where the depth of cut must be accurately controlled to cut through the shroud without puncturing the fuel rod cladding. Prior to the cutting tests, power and speed parameters were obtained by making trial cuts in shroud material until it was just severed; then these parameters were applied to a fixtured shroud-tube combination. For various test conditions and shroud-tube combinations, power was varied from 1.5 to 10 kW, and cutting speed was varied from 50 to 290 cpm.

4.4.2 Gas-jet assist

For effective laser cutting, a gas-jet assist is normally employed to help remove vapors and molten material from the cut formed at the beam impingement point. The jet assist is a small tube positioned to angle its high velocity gas stream at the beam impingement point. Assuming the jet assist and laser beam are stationary, the jet assist is most efficient in removing material when the horizontal component of the gas jet directly opposes the direction of workpiece motion.

The various gas compositions tested included air, oxygen, 50% oxygen--50% nitrogen, nitrogen, helium, and CO₂.

4.4.3 F/number

Laser cutting results are strongly influenced by the f/number of the laser beam-focusing system. The f/number is defined as the focal length of the focusing optics (F.L.) divided by the unfocused beam diameter (D) at the focusing optics ($f/\text{number} = F.L./D$). In general, low f/numbers result in a higher intensity at the focal point, but a shorter depth of field (i.e., beam intensity decreases rapidly as the workpiece location varies from the exact focal length of the focusing mirror). Systems with large f/numbers have a lower beam intensity at the focal point, but a greater depth of field. Experimental results have shown that for most materials less than 6-mm thick, a system with an f/number between 4 and 6 produces the best results. Therefore, a substantial number of the cutting tests were conducted using a 30-cm-focal-length mirror, which resulted in an f/number of 5.3. Also, several tests were conducted using a 46-cm-focal-length mirror (f/number = 9), and a 51-mm-focal-length mirror (f/number = 10) was employed for tests where attempts were made to cut a corner from the hexagonal shroud.

4.4.4 Angle of incidence

Although most tests were run with the laser beam normal to the workpiece surface, several cuts were made with the laser beam axis oriented at a 45° angle to the surface (see Fig. 4.2C). The rationale

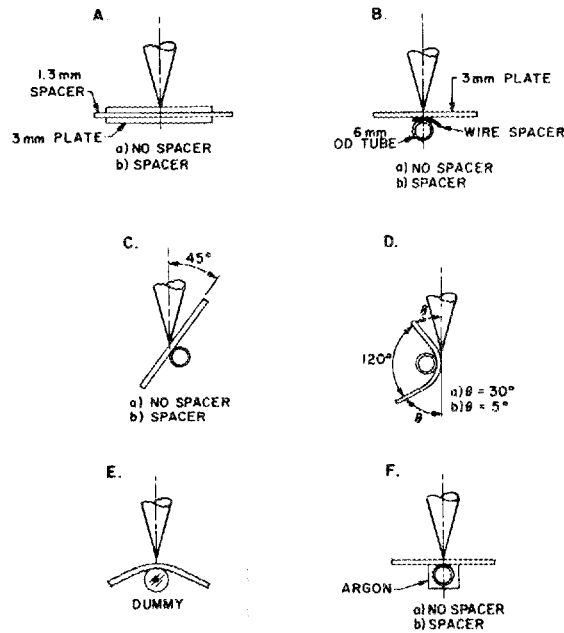


Fig. 4.2. Cutting test configurations.

behind these tests was that the effective wall thickness of the underlying fuel pin tube would be thicker when approached at an angle. However, because of the additional energy required to cut through the (also) thicker shroud, it was not possible to prevent puncturing the tube wall.

Another configuration tested the area where the laser beam axis was oriented at an angle to the shroud surface and involved attempts to cut the corner from the hexagon as shown in Fig. 4.2D. Two different angles (i.e., 5 and 30°) were tested with similar results. When the laser beam broke through the shroud wall, the jet stream was disturbed, resulting in severe damage and the puncturing of the fuel rod cladding.

4.4.5 Beam mode

All cutting tests except the corner cuts were conducted using a laser with unstable resonator optics. As described above, the output beam from unstable resonator optics has an annular shape. This annular beam profile allows the unfocused beam to be turned onto the focusing

mirror and then focused directly back through a hole in the turning mirror, as shown in Fig. 4.3. This focusing arrangement avoids any off-axis aberrations in the focused beam, and therefore, provides a high-intensity spot for cutting. Somewhat higher power was available in the gaussian beam mode than in the annular beam, and so this gaussian beam was chosen to make the corner cuts.

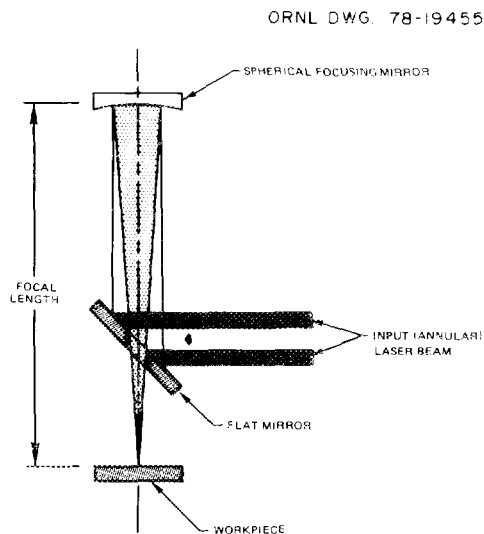


Fig. 4.3. Laser cutting focusing optics.

4.4.6 Purge

Finally, cutting tests were conducted with the space underneath the shroud and around the fuel rod purged with argon, Fig. 4.2. Argon gas readily ionizes in the presence of a high-intensity laser beam and forms a plasma. This plasma absorbs the energy of the laser beam and greatly moderates penetration into a surface underneath it; thus, it was felt that argon might prevent rod puncturing. While this test configuration did not result in rod puncture when rods were wire-spaced from the shroud, the cladding was punctured during direct contact tests.

4.5 Test Results and Discussion

The results of the cutting tests are summarized in Table 4.1. These tests show that cutting cannot be accomplished without penetrating

Table 4.1. Laser disassembly development unit -- laser cutting results
(See Figs. 4.2 and 4.7 for jet-assist configurations and test configurations)

Sample	Test configuration (see Fig. 4)	Power (kW)	Speed (ipm)	Focal length (in.)	Jet-assist configuration (see Fig. 3)	Jet-assist gas	Jet-assist pressure (psi)	Results
NV28-13	A.a	3.5	60	12	A.b	Air	150	Broken apart by hand -- bottom part scarred
NV28-14	A.b	3.5	60	12	A.b	Air	150	Scar in bottom piece
NV29-3	A.b	3.5	65	12	A.c	Air	150	Partial penetration of top plate; slight damage to bottom plate
NV29-16	A.b	5	100	12	A.b	Air	150	Deep scar in bottom plate
NV29-24	A.a	5	115	12	A.b	Air	150	Through in two spots only -- slight holes bottom plate in these two spots
NV29-30	A.a	2	35	12	A.b	Air	150	Bottom plate badly scarred
NV29-31	A.b	2	35	12	A.b	Air	150	Bottom plate scarred
NV29-35	A.b	3.5	70	12	A.a	Air	150	Slight scarring of bottom plate
NV29-36	A.a	3.5	70	12	A.a	Air	150	Bottom plate scarred
NV29-37	B.b	3.5	70	12	A.a	Air	150	No damage to tube -- wire nicked
NV29-38	B.a	3.5	70	12	A.a	Air	150	Plate cut through -- damage to tube one end; tube may not have been in contact with plate
NV30-11	B.b	3.5	75	12	B.a	Air	150	Tube cut through on one end; remainder undamaged fixturing appears not be optimum
NV30-18	B.b	3.5	60	12	B.b	Air	150	Burned through tube where tube directly under beam
DC5-25	B.b	3.0	65	12	B.b	Air	50	Tube cut through in some locations -- new fixture
DC5-33	B.b	1.5	20	12	B.b	Air	50	No penetration through tube wall
DC5-34	B.a	1.5	20	12	B.b	Air	50	Uniform perforation of tube wall
DC6-22	C.a	5	50	12	B.b	Air	50	Severe cutting of tube wall
DC7-21	C.b	5	50	12	B.b	Air	50	Plate not quite cut all the way; one hole in tube
DC8-24	F.b	2	30	12	B.b	Air	50	No damage to tube wall -- wire nicked
DC8-25	F.a	2	30	12	B.b	Air	50	Tube perforated in spots
DC8-36	B.b	2	37.5	18	B.b	Air	50	Tube badly perforated
DC8-37	F.b	2	37.5	18	B.b	Air	50	Tube perforated but not as bad as DC8-36
DC13-7	D.a	10	30	20	C.	Air	50	Through at beginning only -- tube welded to plate wall
DC13-8	D.b	10	30	20	C.	Air	50	Tube badly cut at beginning -- part fixtured on angle
DC13-9	D.b	10	30	20	C.	Air	50	Tube cut through where beam cut through wall
DC14-8	E.	6	100	20	C.	Air	50	One place not cut through all the way; easily broken apart by hand
DC14-9	E.	6	75	20	C.	Air	50	Complete cutting of wall -- piece fell apart in hand
DC20-7	B.b	2.5	30	12	B.b	Air	50	Plate cut through -- slight damage to tube surface but not cut through
DC20-8	B.a	2.5	30	12	B.b	Air	50	Slightly off focus -- penetrated through plate in a few spots only -- holes in tube
DC20-9	B.a	2.5	30	12	B.b	Air	50	Plate cut through -- tube perforated
JN4-23	B.a	2.75	30	12	B.b	N ₂	50	Plate cut through except in a couple of spots -- tube perforated in several spots
JN4-35	B.a	1.0	30	12	B.b	O ₂	50	Tube completely destroyed where beam cut through plate
JN4-39	B.a	2.0	30	12	B.b	50% N ₂ /50% O ₂	50	Plate cut in half -- tube slit in half
JN4-47	B.a	3.5	30	12	B.b	He	50	Plate not quite cut through everywhere -- tube perforated
JN4-52	B.a	2.6	30	12	B.b	CO ₂	50	Plate cut through -- tube slit

a fuel rod that is directly adjacent to the shroud. If the fuel rod is spaced from the shroud by a 1.5-mm wire wrap, cutting conditions can be achieved such that the fuel rod is not penetrated. If a dummy fuel rod can be provided to absorb the laser energy and shield the other fuel rods, a rather wide range of cutting parameters could be used to sever the shroud without affecting any of the fuel rods.

4.5.1 Initial testing

Initial tests, as noted in test configuration A of Fig. 4.2, consisted simply of placing two 3-mm-thick stainless steel plates together, either in contact with one another or spaced by shims. The effect of cutting characteristics on damage to the underlying material was immediately evident as a result of these cursory tests. This is illustrated in Fig. 4.4, a comparison of spaced and unspaced specimens cut at 3.5 kW and 178 cpm. As noted in Fig. 4.4, the unspaced specimen, NV 29-36,

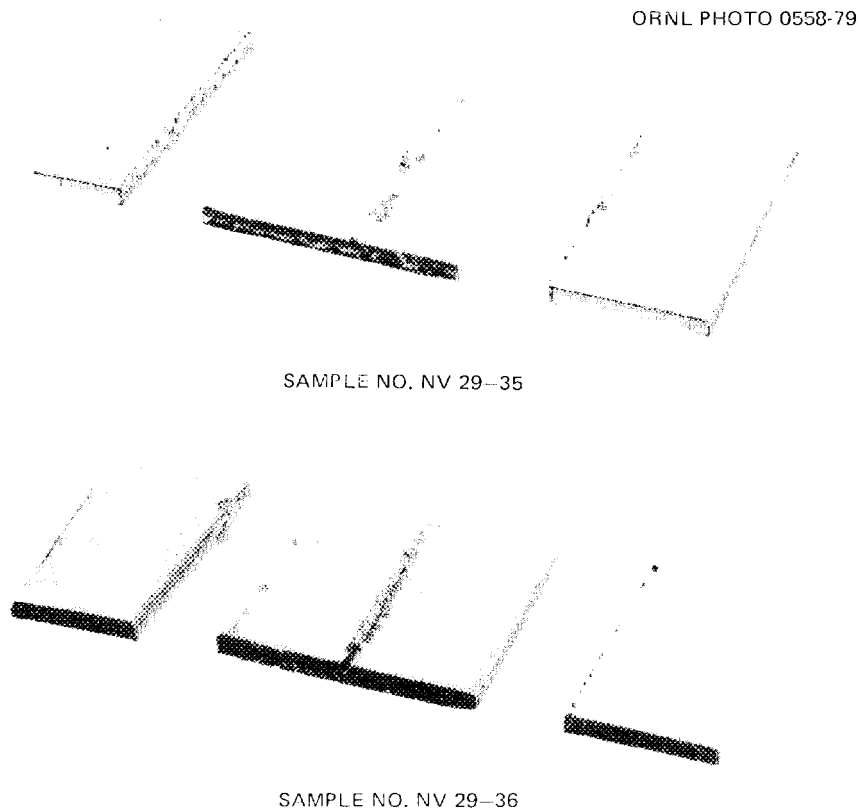


Fig. 4.4. Results of plate-on-plate laser cut.

exhibits a deep scar in the underlying plate, certainly of sufficient depth to puncture fuel cladding. The spaced specimen, NV 29-35, however, is only slightly scarred to a depth which would not penetrate the cladding. As mentioned above, the power-speed combination for both cuts was adjusted to be enough to just penetrate the upper plate thickness.

Following the preliminary plate-on-plate tests, attention was directed toward cutting tests with a plate-on-rod configuration, with and without wire spacers as shown in Fig. 4.2B. Initial plate-on-empty-rod tests were conducted by taping the rod to the plate bottom. This fixturing technique proved to be ineffective because the tube sometimes moved after alignment and was not directly under the beam centerline during the cut. Therefore, the fixture shown in Fig. 4.5 was fabricated and used for the remainder of the tests.

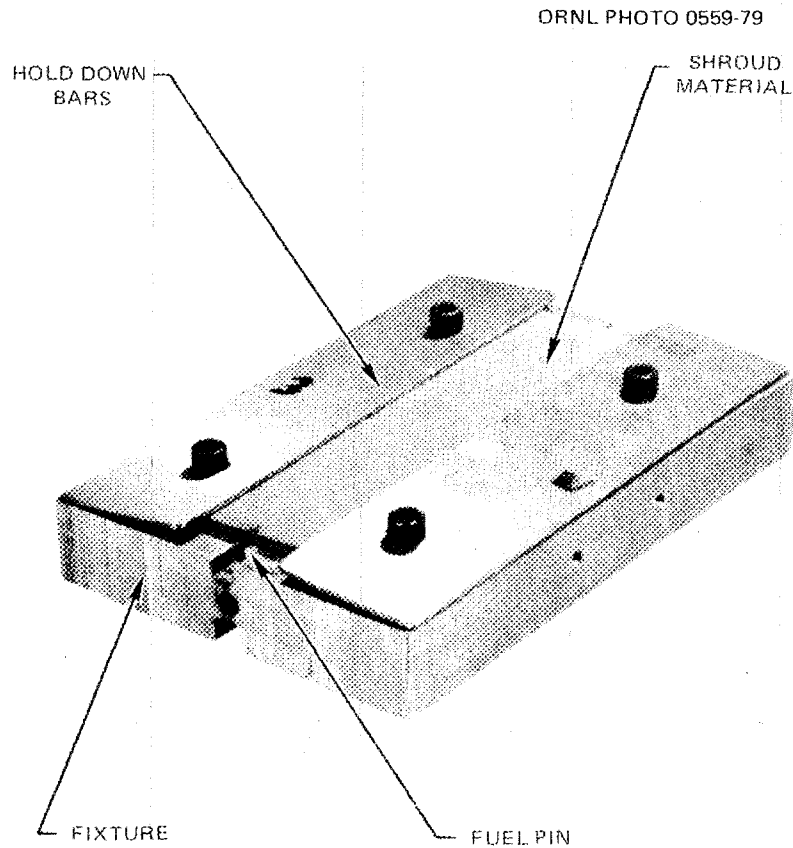
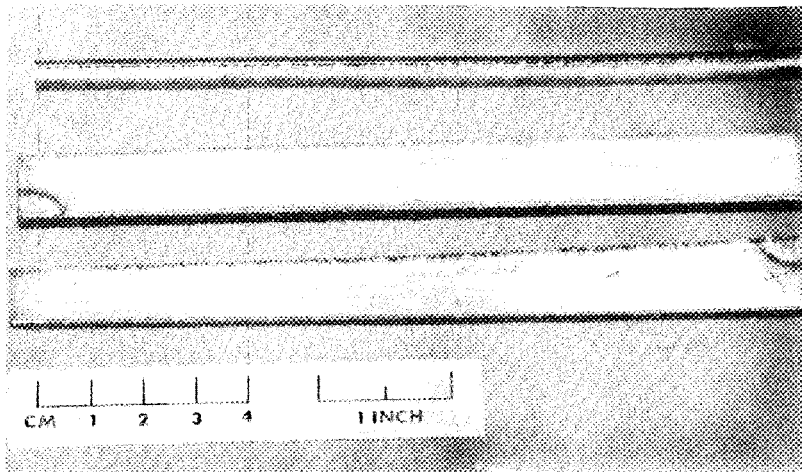


Fig. 4.5. Laser cutting fixture.

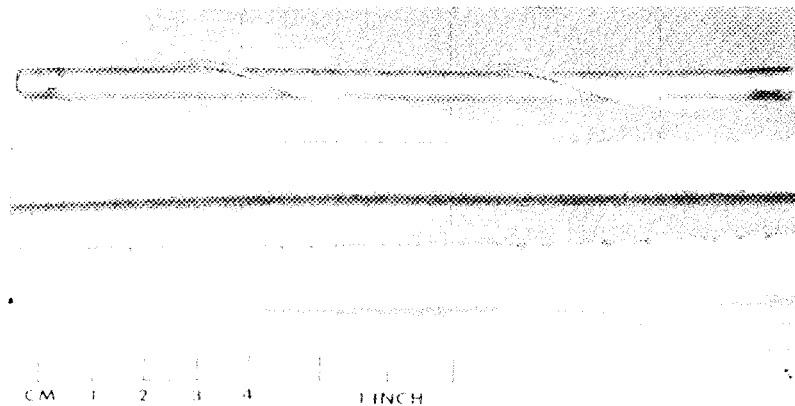
4.5.2 Power and speed tests

Subsequent tests indicated that the least amount of damage to the underlying cladding could be obtained at lower power and speed. Spaced and unspaced specimens (DC 5-33 and DC 5-34) cut at 1.5 kW and 50 cpm are shown in Fig. 4.6. No puncturing of the cladding occurred with the

ORNL PHOTO 0560-79



SAMPLE NO. DC5-34 NO WIRE SPACER



SAMPLE NO. DC5-33 WITH WIRE SPACER

Fig. 4.6. Laser cut specimens cut at 1.5 kW and 50 cpm.

spaced specimen, but the flush (unspaced) cladding was uniformly punctured. Close inspection of the spaced specimen showed that the wire spacer was nicked by the beam and that the tube surface was slightly scarred. This indicates that accurate control of power, speed, and work distance would have to be maintained when cutting through a shroud with wire-spaced rods, because slight changes in these parameters could result in puncturing the cladding or incomplete penetration of the shroud. Based on these and similar test results, it is estimated that speed and power must be maintained within $\pm 5\%$ of set value and that work distance must be maintained within 0.5 mm for a system with an f/number of 4 to 6.

4.5.3 Gas jet-assist tests

As noted in Fig. 4.1, variables associated with the jet assist that were evaluated include diameter, pressure, position, angle of incidence, and gas composition. The different configurations tested are shown in Fig. 4.7. While satisfactory cuts could be obtained with all jet diameters, most of the experimental work was performed using the 3-mm-ID tube oriented at an angle of approximately 30° to the workpiece surface and located 11 mm from the beam impingement point. This configuration allowed the greatest tolerance to small placement errors, and the jet was not fouled by debris emanating from the cut. Smaller diameter jets have the advantage of requiring less gas flow for cutting. However, they do require more accurate placement and must be located closer to the beam impingement point, where they are subject to fouling.

Gas pressure was varied between 0.97 and 7.2 kPa in preliminary tests. No significant cutting advantage was demonstrated at pressures above 2.4 kPa; consequently, most tests were conducted at that pressure.

For many laser cutting applications, it has been found that maximum cutting performance is obtained when the angle between the high-velocity gas stream and the workpiece surface (θ in Fig. 4.1) is maximized. For the present application, where it is desirable to terminate the cutting action after breaking through the shroud material, it was found that a more shallow angle produced better results. An angle of approximately

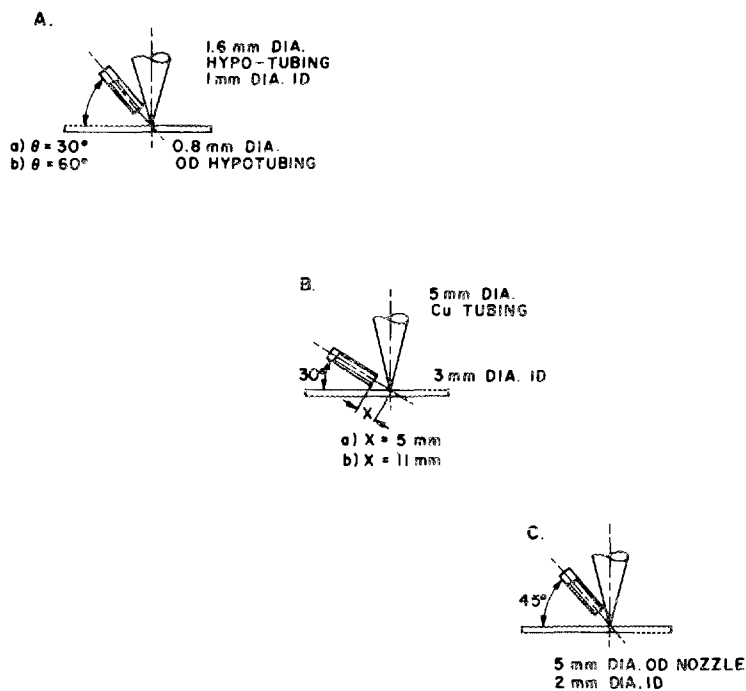
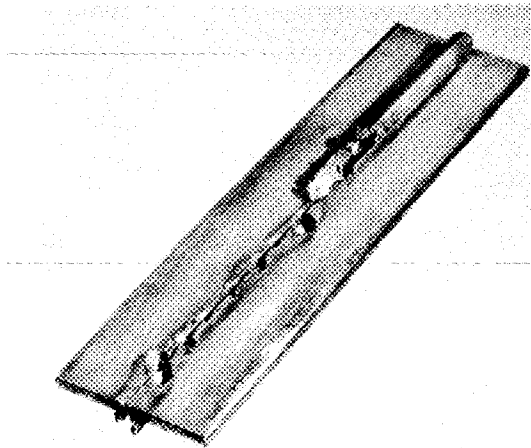


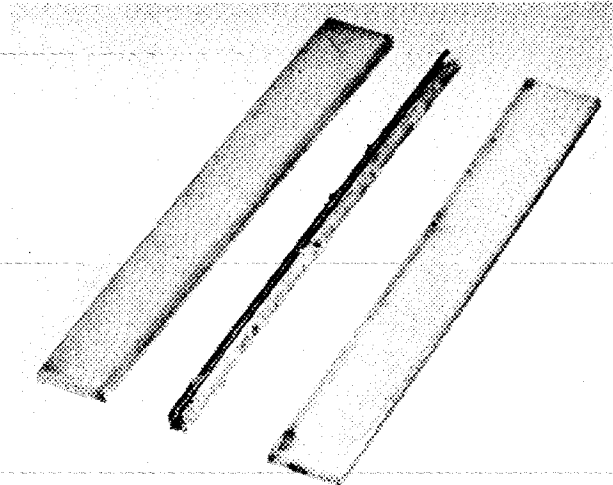
Fig. 4.7. Jet-assist configurations.

30° allowed room for positioning the jet and helped arrest penetration into the fuel rod cladding.

The effect of various jet-assist gases on laser cutting characteristics was also investigated. Most of the cutting studies were conducted using compressed air, since it is inexpensive and is readily available; to add completeness, the cutting characteristics of nitrogen, oxygen, 50% oxygen-50% nitrogen, helium, and carbon dioxide were evaluated. In particular, mixtures of oxygen and nitrogen were evaluated to determine if greater amounts of oxygen would result in a depth of cut that could be more uniformly controlled. For all of these tests a rod directly contacted the plate specimen, as shown in Fig. 4.2B(a). Specimens cut using 100% oxygen, 50% oxygen-50% nitrogen, air, and pure nitrogen are shown in Fig. 4.8. Note that with pure oxygen, the rod was almost completely consumed when the laser beam broke through the overlying plate. This effect is typical of laser cuts using pure oxygen. Although badly damaged, the rod affected by the cut using a mixture of 50%



SAMPLE NO. JN4-35



SAMPLE NO. JN4-33

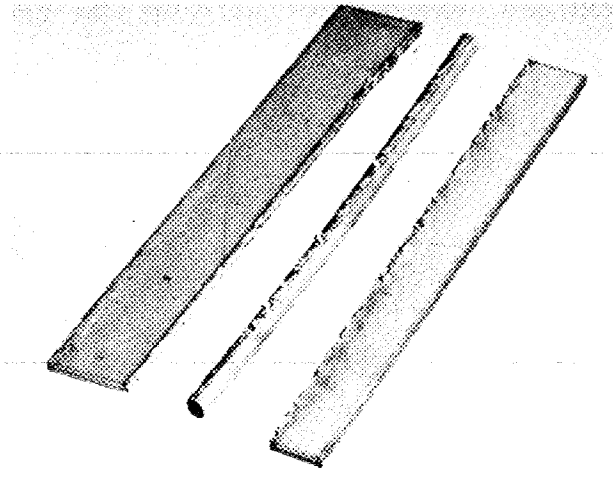
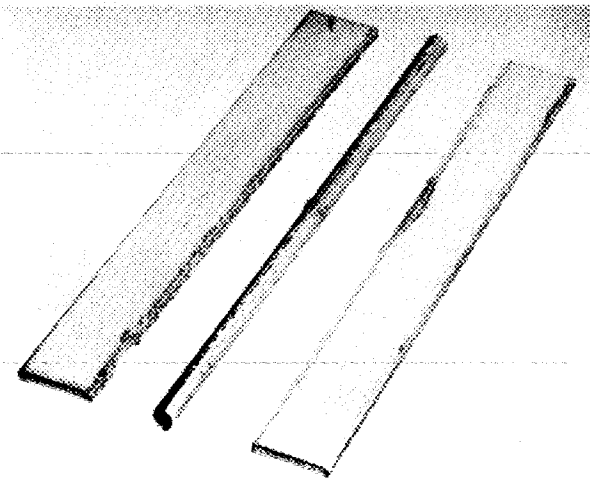


Fig. 4.8. Comparison of laser cuts made with varying amounts of oxygen in jet assist.

oxygen-50% nitrogen was not as badly consumed as the rod affected by the cut with pure oxygen. However, the severe damage to both of these rods indicates the effect of an oxygen-rich cutting gas. Specimens cut using air in the jet assist exhibited uniform perforation of the tube wall as previously described, while the specimen shown in Fig. 4.8 (cut with pure nitrogen) exhibited severe scarring of the tube wall with occasional perforations. Also, the kerf walls of the nitrogen-cut specimen were substantially cleaner when compared to those of specimens cut in pure oxygen or oxygen mixtures. Instead of the characteristic slag at the bottom of the cut, these specimens contained tenacious metal fingers both on the bottom of the plate and on the tube wall.

A specimen cut using carbon dioxide in the jet assist is shown in Fig. 4.9. The perforation or slitting of the tube wall is similar to the results obtained in air, with the exception that the kerf walls were substantially cleaner and much less slag exists at the bottom of the cut.

The specimen cut using helium gas (Fig. 4.10) required substantially more power at the same cutting speed than was required for specimens cut

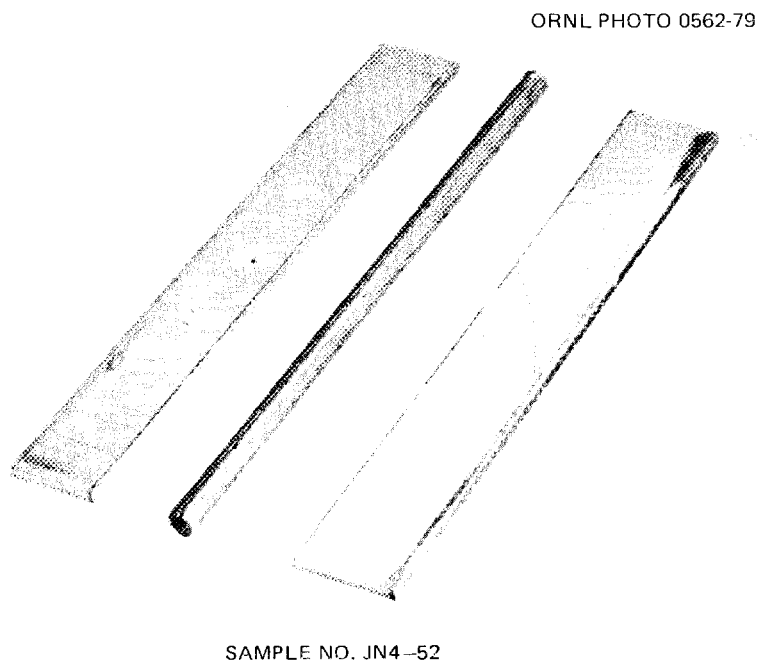


Fig. 4.9. Laser cut using CO₂ jet assist.

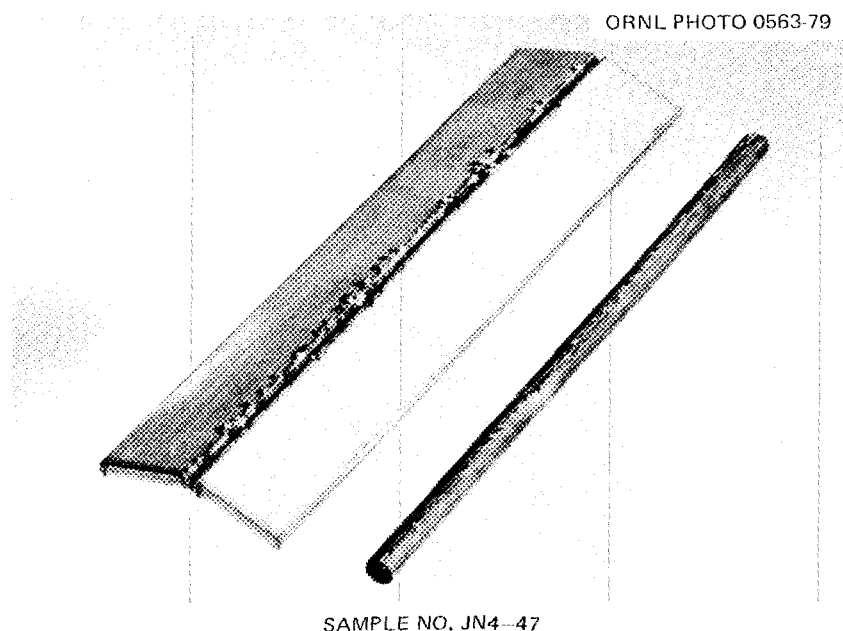


Fig. 4.10. Laser cut using He jet assist.

using other gases; even though the tube was severely perforated, the plate was not completely severed.

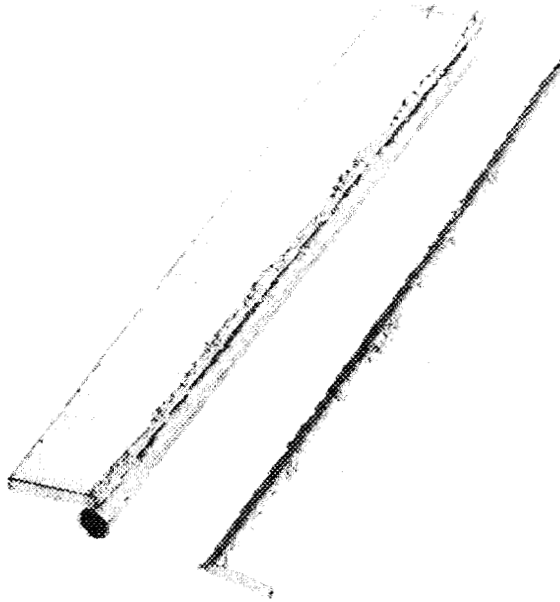
4.5.4 Focal length test

Cuts made using an 18-in.-focal-length mirror ($f/\text{number} = 8$) did not produce satisfactory cutting results. In fact, specimens cut with the rod wire-spaced from the plate could not be cut without perforating the cladding, even when argon was added in the spaces between the rod and the plate.

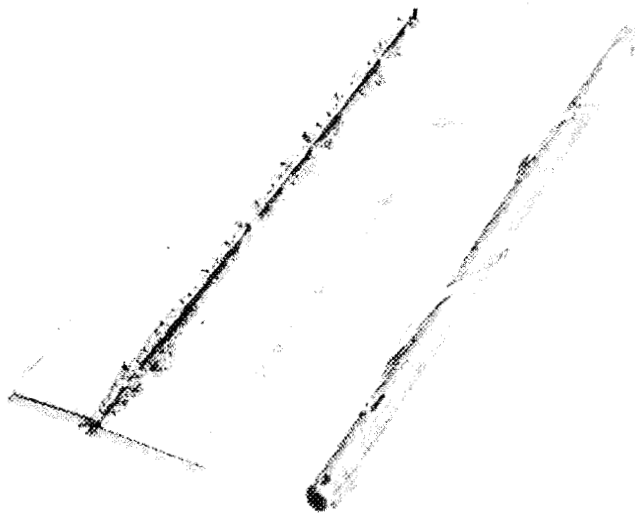
4.5.5 Incident angle tests

Figure 4.11 shows specimens which were cut with the laser beam centerline making a 45° angle to the shroud surface (i.e., test configuration C, Fig. 4.2). The fuel rod cladding in specimen DC 7-21, which was spaced, was punctured in one location, even though the cutting parameters were marginal for completely severing the shroud material. Specimen DC 6-22, where the rod was in contact with the plate, indicates severe cutting through the cladding; in addition, the rod was welded to

ORNL PHOTO 0564-79



SAMPLE NO. DC6--22



SAMPLE DC7-21

Fig. 4.11. Specimens cut with the laser beam oriented at 45° to the plate surface.

one piece of the severed plate. As noted in Table 4.1, more power was required for this type of cut because the actual thickness is 1.414 times the plate thickness for a 45° angle. This greater amount of power results in higher power exposed to the cladding upon breaking through the shroud material and thus a more severely damaged rod.

4.5.6 Corner removal test

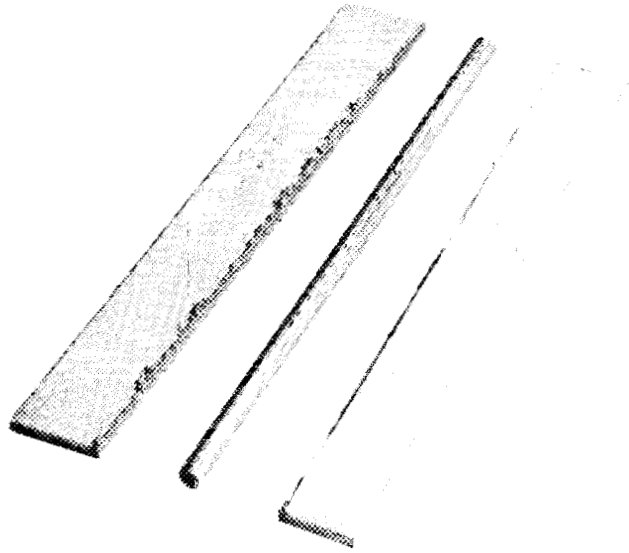
Several cuts were made in specimens fixtured as shown in test configuration D, Fig. 4.2, to determine the feasibility of cutting the corner off the hexagonal shroud. Since these tests involved cutting through a relatively thick section (i.e., >12 mm), a laser capable of higher power was utilized for these tests. The materials-processing area coincident with this laser was equipped with a 51-mm, off-axis, 90° parabolic mirror with an equivalent f/number of 8. A larger f/number system is desirable when cutting through thicker material, because the beam intensity remains constant over a longer distance. Attempts were made to position the beam so that it would cut the hexagon corner and just graze the rod located in the corner. It was found that the corner of the hexagon could be cut; however, as soon as the cut broke through the inner wall, slag buildup would occur inside the shroud and disturb the jet-assist flow. Also, slag would stick to the rod surface and make it difficult to remove the rod from the shroud without rod damage. Finally, beam alignment using this technique was very critical. When the laser beam was not directed close enough to the inside of the shroud, it would slice a section off the hexagonal corner without severing the shroud. When the beam was directed just a little too close to the inner section of the shroud, the rod located in the hexagonal corner would be destroyed.

4.5.7 Argon purge tests

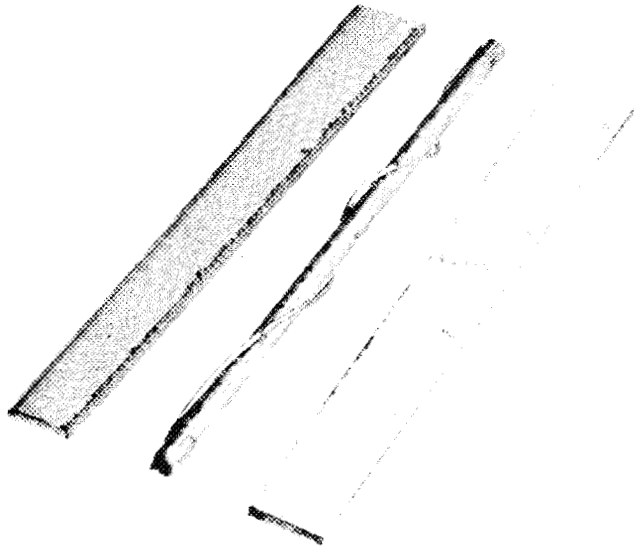
A high-intensity focused laser beam ionizes argon more readily than air, and an energy-absorbing plasma is formed as a result of this ionization. Specimens cut using argon gas in the space between the fixtured plates and rods (test configuration F, Fig. 4.2) are shown in

Fig. 4.12. Power and speed parameters were 2 kW and 76 cpm respectively. The wire-spaced specimen exhibits very slight occasional pitting of the

ORNL PHOTO 0565-79



SAMPLE NO. DC8-25 NO WIRE SPACER



SAMPLE DC8-24 WITH WIRE SPACER

Fig. 4.12. Laser cut specimens with argon gas between the fuel pin and shroud wall.

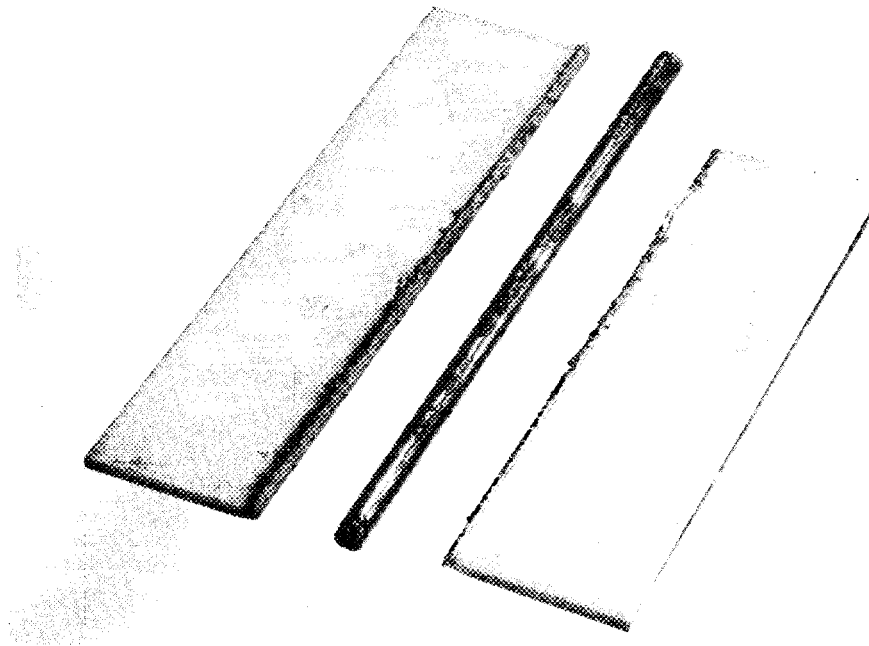
cladding with the wire spacer being nicked approximately 0.3-mm deep in locations which were in contact with the plate. The unspaced specimen exhibited erratic puncturing of the cladding with one 3.8-cm section where the cladding was badly scarred, but not punctured. Thus, it can be seen that the introduction of argon gas in the space between the cladding and the plate absorbs some of the laser beam energy after the plate has been severed, but cannot absorb sufficient energy to prevent puncturing the cladding when it is in contact with the plate.

4.5.8 Dummy rod test

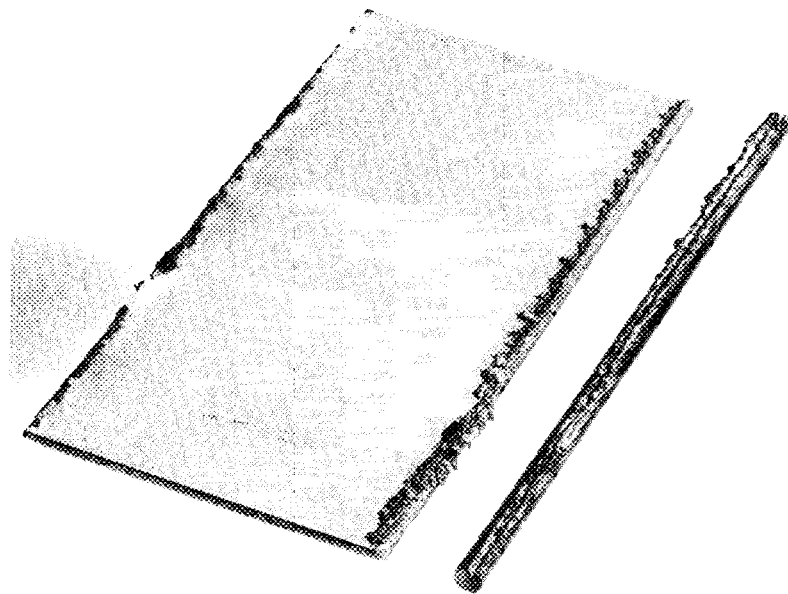
Cutting tests using test configuration E of Fig. 4.2 were conducted to illustrate that, should a dummy steel rod be located in one corner in place of a fuel rod, the shroud could be cut apart easily with no risk of breaching adjacent fuel cladding. A specimen with two corners, each cut at 6 kW, at 250 cpm, and 190 cpm, respectively, is shown in Fig. 4.13. For cut DC 14-8, the power and speed were regulated so that the beam just broke through the shroud surface. This cut contained one small area where the beam did not quite sever the shroud, but the sample was easily broken apart by hand. For cut DC 14-9, the speed was reduced to 75% of its previous value.

One side of this latter specimen fell away freely, but the other side stuck to the dummy rod. However, the rod was easily pried from the shroud, because it was not welded to the shroud but just stuck as a result of hot slag contact at the rod-shroud interface. Thus, this cutting test illustrated that substantial variance in process parameters could be tolerated if a dummy fuel rod were located in a corner of the fuel assembly shroud.

ORNL PHOTO 0566-79



SAMPLE NO. DC 14--8



SAMPLE NO. DC14-9

Fig. 4.13. Laser cut specimen with solid dummy rods underneath shroud.

5. LASER CUTTING SYSTEM ANALYSES

In an attempt to provide a basis for a rational approach to the design of a laser disassembly system for use in a hot cell, certain analyses were made. Among these were consideration of (a) the method of focusing the laser beam and guiding it onto the shroud surface, accounting for the variations in bow and twist of each individual subassembly, (b) operational problems and design approaches to a CO₂ laser beam optical train to operate in the hot cell environment, and (c) the heat and mass flow contributions to the cell environment due to the laser cutting system. Finally, a number of auxiliary design requirements were reviewed while developing a conceptual design of a laser disassembly system. These areas are discussed below.

5.1 Focus Head Control Schemes

The method of directing the focused beam onto the randomly deviating shroud surface requires a basic design. Five types of sense-and-focus methods were studied by comparison to determine their relative merits regarding accuracy, reliability, durability, and cost.

5.1.1 Full length data storage

In this method the position of the fuel subassembly is sensed and stored for subsequent control of the focus head. The z (vertical) and y (lateral) coordinates of the complete cutting path are sensed, and the data are stored for subsequent control of the drive motors for the focus head. One approach would employ an optical scanner, or other remote sensor such as a vidicon tube, to "look" at the entire subassembly to determine the path the focus head should take before cutting is initiated. Alternately, the same data could be obtained from a sensor assembly that is moved along the subassembly axis and is shifted vertically, horizontally, or rotated to maintain a fixed spatial relationship relative to the subassembly. For sensors that do not physically contact the work, such as optical, capacitive, or inductive, the sensor assembly must be driven by z, y, and θ motors under the command of signals from the

sensors. Fluidic sensors or rollers that follow the work mechanically do not require drive motors.

The advantages of this type of data storage are that accurate determination of the cut location can be made without interference from the operation, and the position of the impingement point can be measured directly at the point to be cut. The disadvantages are that (1) the open-loop system cannot compensate for changes due to temperature distortion or mechanical relaxation after the input scan, (2) extremely complicated and expensive data processing is required, and (3) all three axes, and possibly rotation, must be driven by actuators.

5.1.2 Partial length data storage

A second method is to suspend a shroud-sensing unit off the front of the focus head to sense the location of the shroud just ahead of the cutting beam. Information on the shroud position is briefly stored before it is used to actuate the focus head into the proper position.

The advantage of this method over the full-length data storage method is that it would not be affected if the subassembly were to change position during the cutting operation.

5.1.3 Open-loop control

A variant to the second method, which would eliminate the necessity for data storage, involves measuring the shroud location immediately ahead of the cutting beam and using the position information thus derived to directly drive the focus head. This would be an open-loop control system. The primary disadvantage of this method is the possibility of interference from the cutting operation.

5.1.4 Closed-loop control

A closed-loop or boost method could be used. In this approach the sensor assembly moves with the focus head and sensing occurs simultaneously with the cutting operation. Corrections to the focus head location are continually supplied by the sensors to give a closed-loop

control system. No data storage is required, and a continuous, accurate control can be maintained. However, sensing cannot be done directly at the cut, and interference from the process could occur.

5.1.5 Mechanical control

A final method is a direct drive arrangement in which mechanical sensors are used, and the sensor assembly is tightly coupled to the focus head. The focus head is moved in the vertical and lateral directions by forces transmitted from the fuel subassembly surface. No data readout, sensor signals, or drive motors are required, making this method the most reliable, durable, and possibly the least expensive of any of the methods proposed. The only uncertainty is whether the forces required to guide the focus head are too great to be imposed on the fuel subassembly. The weight of the head can be counterbalanced and anti-friction bearings can be used throughout the device to minimize these forces, but these inertial forces required to follow the rod at the proposed cutting speeds are expected to be negligible.

If, however, the fuel rod can tolerate no forces, a closed-loop boost system would be the best substitute for the direct-drive system.

5.2 Shroud Surface Sensors

Optical, capacitive, inductive, fluidic, and mechanical type sensors were considered in this study to track and sense variations in the shroud location. All are assumed to maintain a fixed-spatial relationship relative to the subassembly as they are moved axially along the x axis of the subassembly. The optical, capacitive, and inductive sensors must be driven vertically (z axis) and laterally (y axis), as well as rotated (θ axis) in response to signals from the sensors so that a null reading can be effectively maintained. The fluidic and mechanical sensors can be guided by the subassembly itself and thus exert slight forces on it.

5.2.1 Optical sensor

The optical sensor, as shown in Fig. 5.1, requires a small-diameter collimated light source and a grid of light-sensitive detectors arrayed axially and laterally above the subassembly. The light beam source is directed downward at a slight angle off the normal of the subassembly surface where the cut is to occur (Fig. 5.1a). Vertical standoff is maintained when the reflected beam is axially displaced by a distance proportional to the separation between the surface and the light source. The lateral detectors sense this displacement and, through signal processing and drive motors, adjust the vertical height of the light source to maintain the reflected beam at the correct lateral location. Lateral displacement of the subassembly relative to the light source causes a lateral displacement of the reflected beam in the opposite direction because of the surface curvature at the impingement point, as shown in Fig. 5.1b. The light source is driven laterally (y axis) as required to restore the reflected beam to the correct detector. Any twist of the subassembly (θ axis) is not important, because the path of the sensor inherently defines the line where the cut will occur (i.e., where the surface is normal to the focused beam).

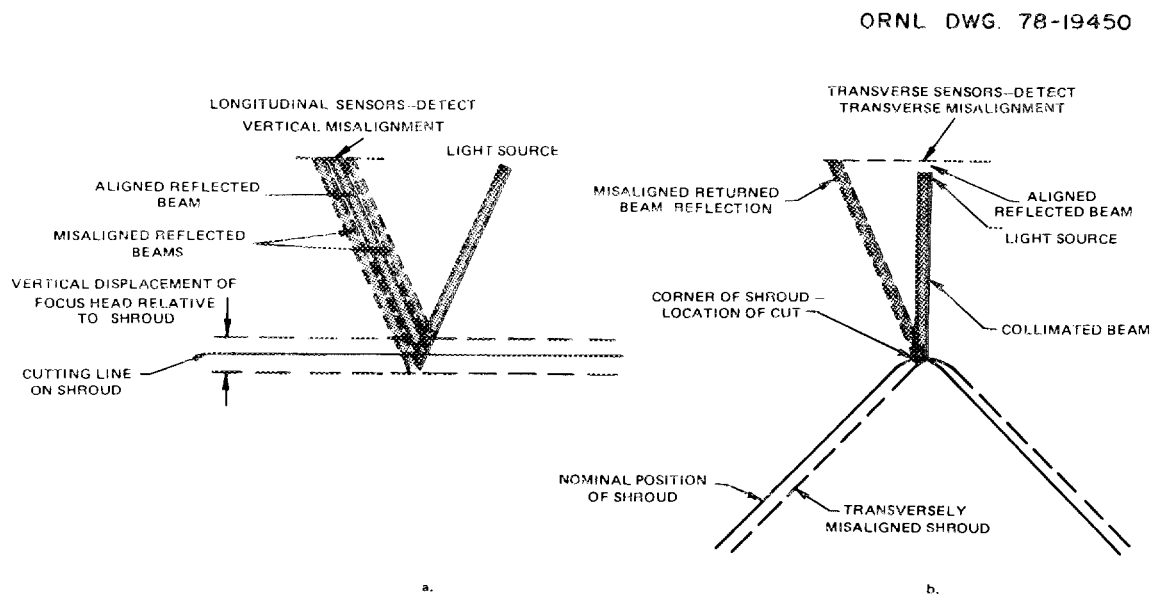


Fig. 5.1. Optical sensor technique.

A single optical sensor can measure two axes, all the required information for control, without inducing stress on the fuel subassembly. Fiber optics are required for both the light source and sensor in order to remove the relatively complex opto-electronic package from the radiation environment. Optical sensors are somewhat delicate, and the reflected beam can be affected by surface scratches, dents, and variations in the surface reflectivity. Finally, signal processing and drive motors are required for optical control.

5.2.2 Capacitive or inductive sensors

Capacitive or inductive sensors could be arranged as shown in Fig. 5.2, with a sensor on either side of the subassembly. These sensors would locate the surface laterally and a sensor on either side of the apex (where the cut would be made) would determine the vertical location and the twist of the subassembly. The sensor assembly would be rotated until the two top sensors were equidistant from the surfaces and adjusted vertically to a predetermined clearance. The assembly would simultaneously be adjusted laterally to give equal spacing from the surfaces. Changes in lateral dimensions would not affect the centering process.

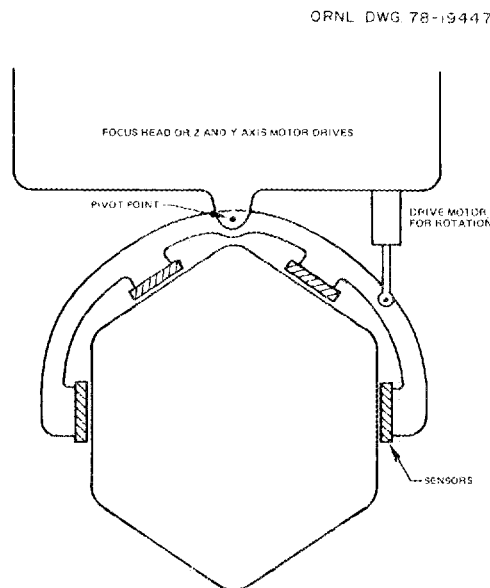


Fig. 5.2. Capacitive or inductive sensor technique.

An ac signal would be applied to the sensors, and the differences in capacitance or inductance would be detected by bridge circuits located remotely from the sensors. Drive motors would then be activated by the processed signals. This system uses signals to detect, transmit, and process, with relative ease and can be used on a real-time basis in the plane of the focus head. However, capacitive pickups may be affected by the ionized gases that result from radiation and the cutting process. Again, drive motors would be required for the sensors.

5.2.3 Mechanical sensor (rollers)

Rollers could be arranged around the corner (to be cut) and on the opposite corner, with the lower set being spring-loaded, to account for subassembly swelling. The upper rollers would be rigidly attached to the roller assembly, which, in turn, would pivot about the focal point of the cutting beam. The location of this pivot point could be either (1) recorded for open-loop drive, (2) attached directly to the focus head to guide it along the subassembly with no drive motors required, or (3) used as part of a closed-loop boost system (to be described in the next section).

This is a very simple continuous control technique that can provide accurate following of the surface without auxiliary guidance. It has the ability to drive the focus head directly without being affected by either radiation or the cutting process. However, the primary disadvantages are that some load is induced by the rollers on the surface, and real-time control is impossible because the rollers cannot track exactly in the focal plant.

5.2.4 Fluidic sensors

Back-pressure fluidic sensors are essentially miniature "ground effect" machines between 12 and 25 mm in diameter. They resemble bottle caps with a gas feed line, and force is transmitted from the cap (or sensor) to the work surface through a cushion of air (or gas) between the two, as shown in Fig. 5.3. With a fixed gas flow, the force between the surfaces varies inversely as the square of the separation between

ORNL DWG. 78-19448

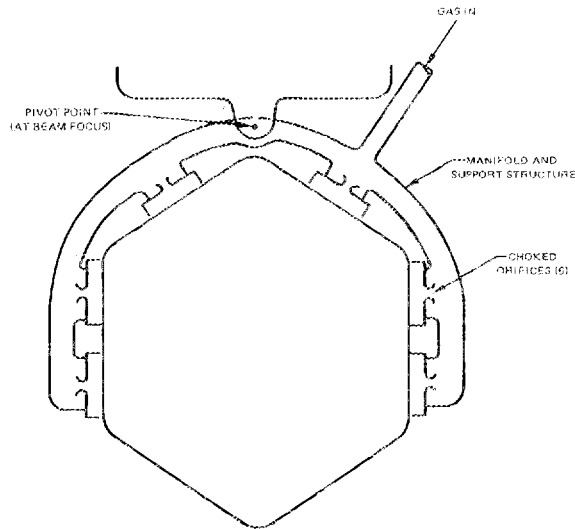


Fig. 5.3. Direct drive fluid sensor technique.

the surfaces. Thus, the fluidic sensors act similarly to rollers mounted on nonlinear springs, and consequently, will follow the position of the subassembly without additional driving forces.

The fluidic sensor is particularly well-suited to a closed-loop drive system, and the focus head can be driven directly by the sensor assembly with no auxiliary guidance. In addition, imperfections or bulges on the surface should not cause erratic operation because of the 3- to 4-mm clearance between the sensors and the surface of the subassembly. However, careful selection of parameters must be made to avoid instabilities. Also, 90 to 140 lps of gas at 140 to 210 kPa would be required to operate these sensors.

5.3 Selected Focus Head and Sensor Systems

Based on the options presented above, a system employing a focus head driven directly by a follower using rollers was selected for the design phase of this study. The mechanical details of this system are described in Sect. 6, and demonstrations of these focus head and follower concepts are the primary actions recommended for the future work on a laser disassembly unit.

In the evaluation of the alternate systems, it was pointed out that the mechanical follower would exert some force on the fuel subassembly,

which may compromise the operation of that system. If the mechanical system becomes unacceptable, the second-best system would be that employing a closed-loop, or "boost" control system. The following discussion concerns that approach and its possible implementation with different follower types.

In the closed-loop, "boost" control system, the sensor assembly moves with the focus head, and motion is controlled by error signals originating from the sensors. With optical, capacitive, or inductive sensors, the sensor assembly would be rigidly attached in the x, y, and z axes, but would be free to rotate in the θ direction about the focal point of the cutting beam. This rotation would permit the sensor assembly to follow the twist of the subassembly and would be affected by an auxiliary drive motor or piston controlled by the sensors. The y and z axes (lateral and vertical to the fuel subassembly longitudinal axis) would also be driven by either electric motors or hydraulic or pneumatic pistons under sensor control. The x axis (longitudinal) would be independently driven by an electric motor and controlled by a mini-computer, according to a predetermined schedule of cutting speed and laser power.

When using mechanical rollers for the sensors, the roller assembly would be attached to the focus head through an orthogonal pair of appropriate control devices, such as hydraulic or pneumatic valves. These valves would actuate pistons or electrical transducers to control drive motors. The drive motors or pistons would be energized as required to maintain the focus head at a null position relative to the sensor assembly.

The use of valves in conjunction with hydraulic or pneumatic drive cylinders would essentially eliminate all signal processing and obviate the need for electric motors.

Fluidic sensors can also be used to follow the fuel subassembly and drive the focus head directly if the side and vertical loads are not greater than a few pounds. This type of sensor is uniquely suited to a boost configuration, as it can act both as the sensing element and as the control valve. A possible configuration, shown schematically in Fig. 5.4, consists of four sensors and three pneumatic cylinders. Gas is fed to both sides of the lateral (upper left) cylinder through choked

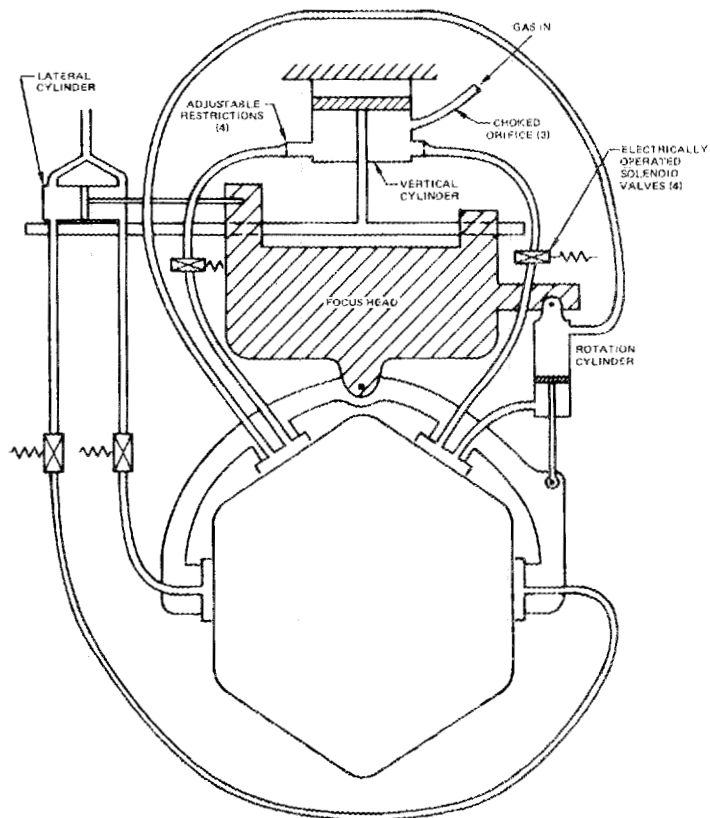


Fig. 5.4. Fluid sensor boost arrangement.

orifices to ensure a fixed flow rate. The two side sensors are also connected to the cylinder through flexible lines containing variable restrictions to adjust the flow for optimum performance. If the shroud surface is closer to the right sensor than the left, the leakage rate at the right sensor will decrease, thereby increasing the pressure in the left side of the lateral cylinder. The cylinder will then force the focus head and sensors to the right until equal leakage rates and equal spacings are obtained. The vertical sensors operate in the same manner, but additional gas lines (to sense differential pressure) are connected to a third cylinder. If the subassembly is twisted relative to the sensor assembly, the differential pressure between the two upper sensors will cause the rotational cylinder to rotate the focus head to the desired alignment.

The focus head would be counterbalanced to reduce the vertical load on the boost system to between 2.5 and 4.5 kg, which is sufficient to provide the maximum vertical acceleration required.

For initial positioning of the sensor assembly, electrically operated solenoid valves would be inserted in the lines. Closing either side valve would drive the assembly laterally until it was positioned over the rod. Opening both upper valves, the assembly would then be lowered into position. At the end of the cutting sequence, the upper valves would be closed, and the unit would ascend vertically for return to the starting location.

5.4 Optical Components

This study was originally intended to address only the in-cell beam transfer and focusing optics and the special problems caused by the radioactive environment. However, recognizing that the problem of beam transfer from outside the cell to inside the hot cell must eventually be confronted, some preliminary consideration was also devoted to the window problem area. Discussion of these two areas, in-cell optics and the beam transfer window, follows.

5.4.1 Laser optics in the hot cell

In general, there are two basic classes of optical components suitable for use with multikilowatt carbon dioxide laser beams. These are (a) reflective optics (i.e., front surface mirrors), constructed either of metal or coated semiconductors, or (b) refractive optics (i.e., lenses or prisms), constructed from an alkali halide or zinc selenide. Refractive optics suitable to this application are limited in terms of suitable materials for construction. The requirement for transmission of almost all of the incident 10.6 μm radiation limits the choice to the alkali halides, zinc selenide, germanium, cadmium telluride, and a few other materials. The problems encountered with multilayered semiconductor or alkali halide mirror coatings are essentially identical to those encountered by refractive components. However, the usage of

the reflective metallic mirror is by far more general in industrial carbon dioxide laser systems because of its lower cost and higher damage resistance, and is therefore preferred for use in the hot cell.

The simplest physical model of a metallic mirror in operation is to consider the laser beam as an electromagnetic plane wave traveling through a dielectric medium and striking the surface of a perfect conductor. Maxwell's equations provide a direct solution which predicts that the reflected wave leaves the mirror at an angle equal to the angle of incidence (in classical optics, this is Snell's law), and a sheet current flows at the surface of the metal in proportion to the magnetic induction tangential to the surface. In the real-world case of finite conductivity, the solution becomes complex; it suffices to point out here that electric fields exist inside the metal surface. These electric fields produce currents, which, in the presence of a finite conductor, cause some of the incident power to be absorbed. The physical cause of finite conductivity results from the interaction of the free electrons in the metal with the crystal lattice. Numerous mechanisms have been shown^{9,10} to influence the electrical conductivity, such as electron collisions with the lattice, lattice imperfections, and impurities. Resonant or quasi-resonant phenomena can also occur between the electrons and the normal vibrational modes of the lattice. Thus, any damage in a metal mirror as a result of x-ray induced Compton scattering or electron-positron pair production, should affect the conductivity when the induced defects approach the natural defect level of the metal used. However, in the case of metals at room temperature, the conductivity is controlled by impurities.⁹ It seems unlikely that the x-ray environment would lead to any intrinsic increase in the absorption of a metallic mirror. Extrinsic mechanisms, such as surface contamination with dust, dirt, and vapors, could be a significant problem. In nonnuclear environments, this has shown itself to be the limiting factor in controlling mirror life.

Two basic modes of mirror failure are of interest in analyzing the system. The first is catastrophic failure, in which the mirror absorptivity becomes so high that the beam actually melts or pits the mirror.

At the flux densities and power levels of the system in question (i.e., 2 to 3 kW in a 75-mm-diam beam), this could come about only if a strongly absorbing material were brought into contact with the mirror face. Protection of the mirrors from this mode of failure requires that the mirrors be protected from dust, dirt, metal chips, grease, oils, etc. This can be done by enclosing each mirror in a purge box and introducing a flow of clean air or nitrogen to keep the mirrors dust-free. The second and more subtle mode of failure consists of a change in the optical properties of the mirrors as a function of time. This is caused by slow increases in mirror surface absorptivity of laser radiation, inducing heat, which produces thermal stresses. These thermal stresses cause mirror deformation and aberrations that change the focal plane position. This type of effect is very slow, and regular use of a calibration station (to test the beam-cutting capability before cutting each assembly) should provide control of the very gradual drift in focal plane position.

In order to determine if, in the hot cell environment, it is possible to make use of uncooled mirrors for the focus head, two separate sets of calculations were made. The first is a heat flow calculation, which determines the rate of temperature increase of the mirror substrate when it is irradiated by a laser beam. The second is the determination of mechanical deformation of the mirror, caused by the calculated temperature distribution. These calculations were performed using computer programs previously developed at the United Technologies Research Center for laser mirror analysis.¹¹

For the calculations, the mirror considered was made of solid copper, 5-cm thick and 10-cm in diameter. It was illuminated by a 7.5-cm-diam, 5-kW, 10.6- μ -laser beam, with an inside (no power) diameter of 38 mm, corresponding to a beam magnification of 2. A mirror surface absorptivity of 0.01 was assumed. This is a relatively conservative value for copper, which, normally, under freshly polished conditions, is approximately 0.005. An absorptivity of 0.01 means that 50 W of the incident radiation is absorbed at the surface of the mirror. A computer code, which determined the temperature at the surface and at points

within the mirror, was employed to calculate the temperature distribution in the mirror blank for a beam-on time of 120 s.

Two cooling mechanisms were assumed to operate during this 120-s period. The computer code automatically calculates the free convective heat transfer coefficient for the surface in relation to the assumed air temperature in the room and calculates the heat loss by convection. Radiative cooling was calculated assuming that (a) the spectral emissivity of the copper mirror blank is 0.01, and (b) the mirror is in an isolated uniform absorptivity sphere of temperature 26°C. For 120-s irradiation, starting at a temperature of 26°C, the hottest point on the mirror substrate reached a temperature of 27°C. The highest mirror temperature vs time for this case is shown in Fig. 5.5.

Based on previous UTRC experience with high-power laser mirrors, this small rise in temperature will be insufficient to produce any meaningful optical distortion of the beam. However, for completeness a simple calculation, which grossly overestimates the distortion of the mirror, was made and indicated that the mirror distortion is, in fact,

ORNL DWG. 78-19438

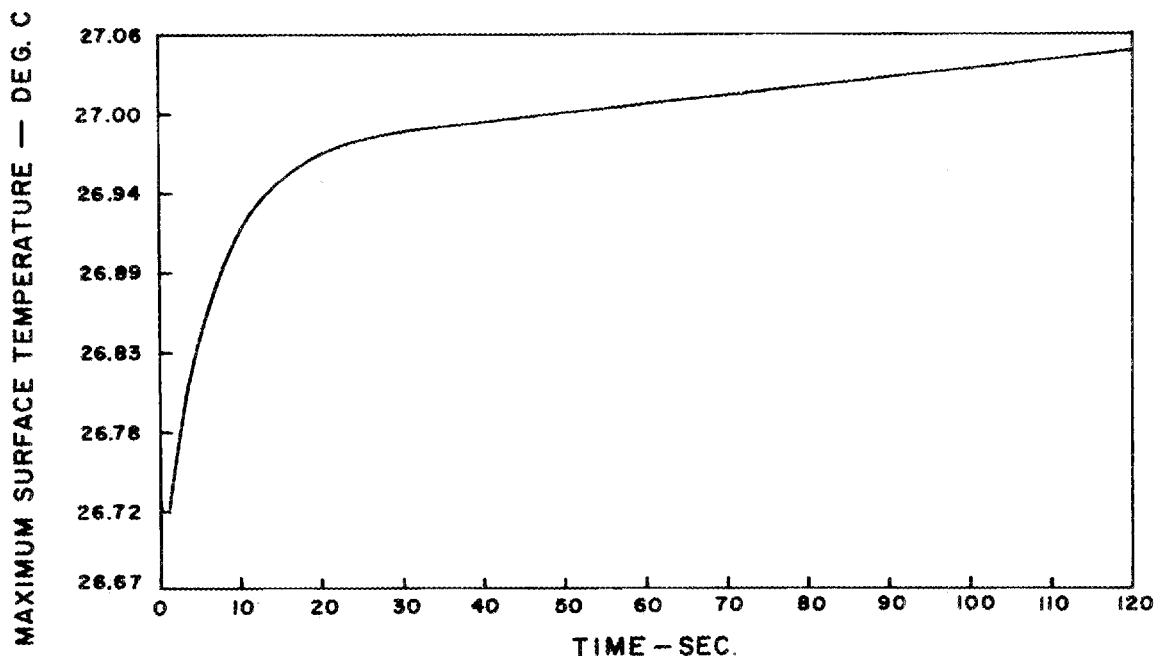


Fig. 5.5. Maximum transfer mirror temperature during beam on-time.

negligible. The total deformation of the mirror was calculated by making the following assumptions: (1) Young's modulus of the mirror material is 0 (mirror has no stiffness), (2) the mirror deforms elastically by thermal expansion under an assumed uniform temperature gradient, and (3) the reflective surface of the mirror has a temperature which is 0.5°C higher than the back surface.

A calculation of the front surface thermal expansion of the 10-cm-diam mirror indicates the front surface diameter is longer than the back surface diameter by 6.4×10^{-5} cm. Since the substrate has no stiffness, it will deform into a section of a spherical shell, because the outer shell is longer than the inner shell by the previously calculated thermal expansion. The induced radius of curvature was calculated and found to be 4.7×10^5 cm. This corresponds to a focal length (of the concave side) of 2.3×10^5 cm. Therefore, each of the flat mirrors in the optical train will become slightly convex. The focusing mirror, which is concave, will become slightly less concave. Because the three flats and the curved mirror are so close together, and the radius of curvature induced by the thermal deformation is so large, the effects can be considered additive; so that the focal length shift calculated for one mirror can be divided by four to obtain an estimate of the shift in the location of the cutting focal point. For an f/7 focusing mirror, the focal length increase, due to this overestimated thermal expansion of the mirrors, is approximately 0.5 mm. This is within the allowable tolerance for effective cutting. Exact calculations of the mirror deformation, in which allowance is made for physical stiffness of the mirror, can be expected to indicate a focal length change of the curved element, which would be between 1/2- and 1-order of magnitude less than that estimated here.

5.4.2 Laser window

Introduction of the laser beam into the disassembly cell requires a window that will allow laser transmission to be constructed from either an alkali halide material or zinc selenide.

Relative to the potential use of either the alkali halides or zinc selenide as a window, it is useful to consider some basic mechanisms

that can cause failure in these solid windows. These materials (a) are all relatively weak, having yield strengths in the range of 2.7 to 41 MPa, (b) have extremely low thermal conductivity, (c) have relatively high expansion coefficients, and (d) show small absorption of 10.6 μm radiation.

Absorption coefficients ranging between 10^{-4} and 5×10^{-3} are commonplace for these materials. The absorbed power must be conducted through the window to the holder which supports the window. This heat conduction, and the resulting thermal gradient, produce azimuthal hoop stresses in the window. These hoop stresses can lead directly to tensile failure at the outside edge. Reference 12 gives a detailed calculation of the stress levels involved and reports on simple experiments showing the mechanism at work in potassium chloride. At the power levels envisioned for the laser system under study, potassium chloride, sodium chloride, and zinc selenide should be capable of transmitting the beam for long periods of time without damage to the window.

Contamination of the window with metal vapors, dust, or other foreign materials can drastically increase the absorptivity of the window and lead to premature failure. In the case of the alkali halides, considerable work¹³⁻¹⁷ has been done in investigating the mechanical and visible optical effects of radiation damage. More recently Lipson et al.¹⁸ have shown that cobalt-60 radiation, which increases the number of F centers in the material, causes an increase in the absorptivity at 10.6 μm . For radiation doses on the order of 10^7 R, Lipson shows relatively minor increases in the absorptivity of the window. For doses on the order of 2×10^8 R, the increase in the 10.6- μm absorptivity is approximately a factor of 3. This is sufficient to degrade a serviceable window to the point of replacement.

A more advanced type of alkali halide window, which has been artificially strengthened by doping with rubidium, europium, or other materials, unfortunately shows a similar trend. Magee et al.¹⁹ have shown that irradiation with 1-MeV electrons produces an effect similar to that observed by Lipson in pure potassium chloride; that is, the 10.6- μm absorptivity increases as a function of radiation damage. To use an alkali halide window considering the results of Lipson and

Magee,^{18,19} it will be necessary to shield the window from the cobalt-60 radiation. A limiting window lifetime will be reached when the window exposure reaches an integrated value of approximately 10^7 R. Although no direct measurements have been found to date on zinc selenide, it is assumed that a similar process will take place in this material. Lipson and Magee have shown that radiation-induced damage is directly connected with the 10.6- μm absorptivity. Since the absorptivity of the alkali halides and the zinc selenide at 10.6 μm is in both cases a combination of extrinsic absorption (i.e., impurity-induced and multiphonon absorption from the lattice), it seems likely that irradiation of the zinc selenide will produce an increase in the 10.6- μm absorptivity of the material.

Another basic problem with the use of solid windows is resistance to the decontaminating fluids used in the hot cell. The alkali halides are almost completely water soluble. They cannot be exposed even to a relatively humid room (e.g., about 50% relative humidity) without sustaining rapid damage and degradation of the infrared properties of the material. Zinc selenide does not have the water solubility problem. In addition, zinc selenide is reasonably resistant to hydrofluoric acid and some other solvents. Industrial experience has shown that zinc selenide windows typically require cleaning (to remove dust and metal vapor deposits) every 200 h or so to maintain their optical properties.

In summary, the concept of a cell window for the laser beam was not considered as part of this feasibility study, but information indicates that beam entrance to the cell should not create any problem that would prevent the use of a laser for disassembly.

5.5 Laser Heat and Mass Contributions to the Hot Cell

The laser cutting system will introduce heat and gas loads into the disassembly cell. The heat loads to be considered are the laser energy itself, which is eventually deposited in the environment of the cell, the heat energy generated by the motors to drive the optical assembly, and possibly other motors necessitated by the selection of a particular gas-jet generating scheme. In general, these heat loads are insignificant relative to the other heat loads in the disassembly cell.

Assuming a 3-kW laser beam will require five minutes to cut approximately 3.8 m of shroud material, and assuming two cutting cycles per hour, the laser beam will deposit the continuous equivalent of 500 W into the disassembly cell. The drive motor for the focus head will deposit a 20-W equivalent, assuming it is operating at maximum power for the full five minutes of each cycle. A pump motor will put an additional heat load of 730 W on the cell environment. Thus, a total heat load on the order of 1250 W is estimated for the laser cutting system, which is small compared to other heat sources within the cell (e.g., 13,000 W for waste heat from the fuel subassembly).

With regard to the mass balance, the principal mechanism of mass injection into the cell is the cutting jet-assist gas. Basing the calculations on the assumed ten minutes of total cutting time in any given one-hour period, the cutting jet will require an average addition of 1.39 std liters per second of gas added to the cell. This is based on the assumption that an external source of high pressure gas is used to supply the cutting jet. It would also be possible to close-loop the cutting jet by putting a small compressor and gas storage tank in the disassembly cell. Gas from the cell environment could then be pumped to high pressure and used as the cutting jet, thus reducing the gas load on the decontamination systems.

If, as presently envisioned, the ambient environment in the disassembly cell contains oxygen, it can be shown that impact on the cell gas treatment system is insignificant, if not advantageous.

6. SYSTEM DESIGN

Based on the general approach outlined by the analyses discussed in the previous section, preliminary layouts were made of a laser disassembly system for use in a disassembly hot cell. This section contains a description of this system, including four engineering drawings, three isometric sketches, and a system specification.

6.1 Laser Cutting System Description

Shown in Fig. 6.1 is the laser cutting system which is used to cut the outer shroud of a spent fuel subassembly so that the shroud can be removed to expose the inner rods. An isometric sketch of the system is shown in Fig. 6.2.

The system is designed to satisfy the requirements of cutting in a hot-cell radiation environment. Only the "X" carriage, which carries the focus head over the fuel subassembly, is actively driven. The focus head has no drive motors or other electrical components. Its "Y" and "Z" motions, to allow the focused beam to follow the shroud upper corner, are controlled by mechanical shroud followers which track the shroud surface during circumferential and longitudinal cutting. Mirror alignments and replacements are designed to be accomplished from a vertical position with remote manipulators. The total system consists of the following assemblies:

1. a 3-kW laser;
2. a hot-cell window for passage of the laser beam through the cell wall;
3. a gantry assembly with support structure, "X" axis carriage and drive system, "Z" turning mirror, and rest station;
4. the focus head assembly;
5. the shroud follower assembly with circumferential and longitudinal followers; and
6. the calibration station.

The first two items, the laser and the hot-cell window, were not the subject of design in this study. The other items in this list are discussed below in turn.

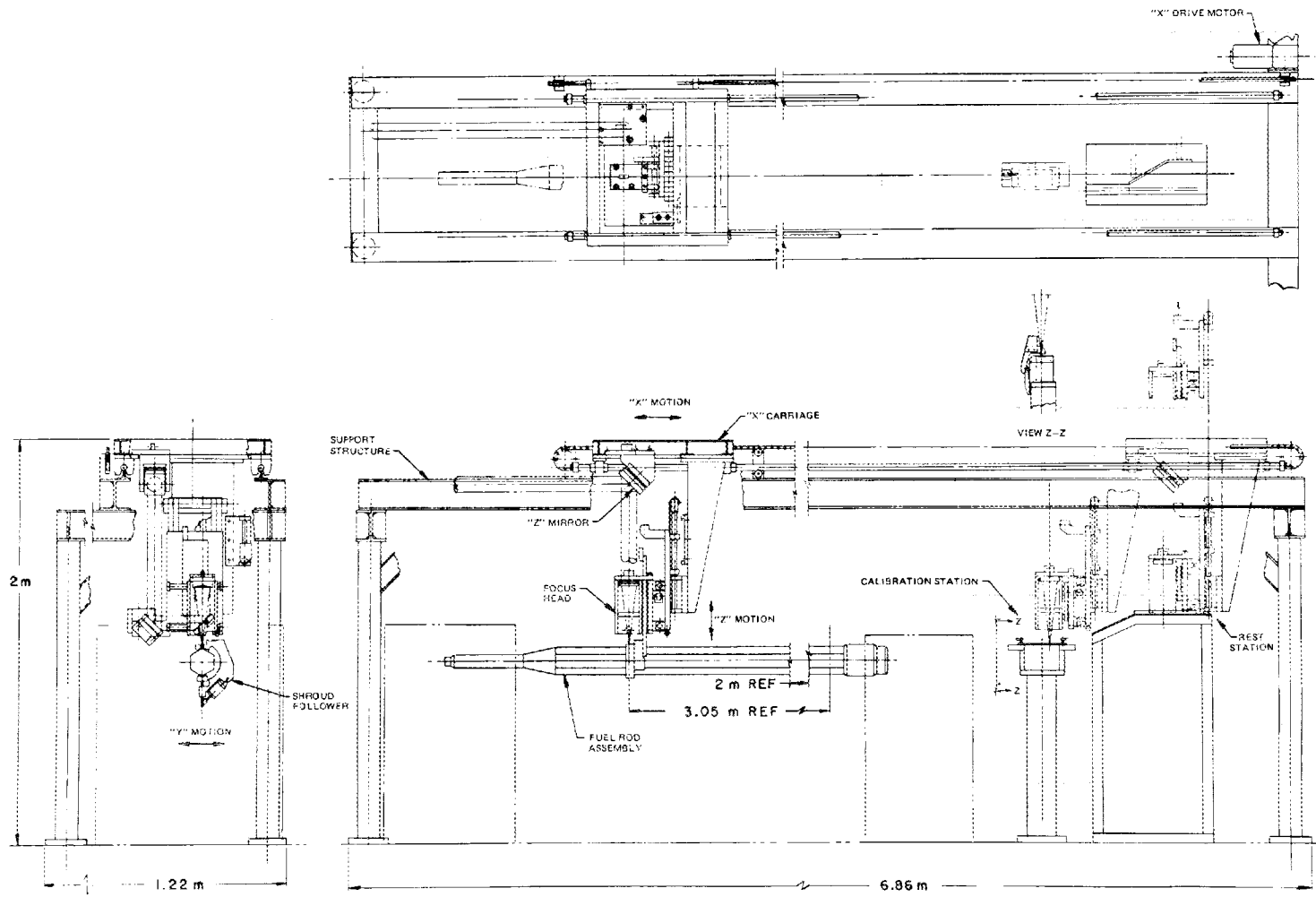


Fig. 6.1. The laser cutting system.

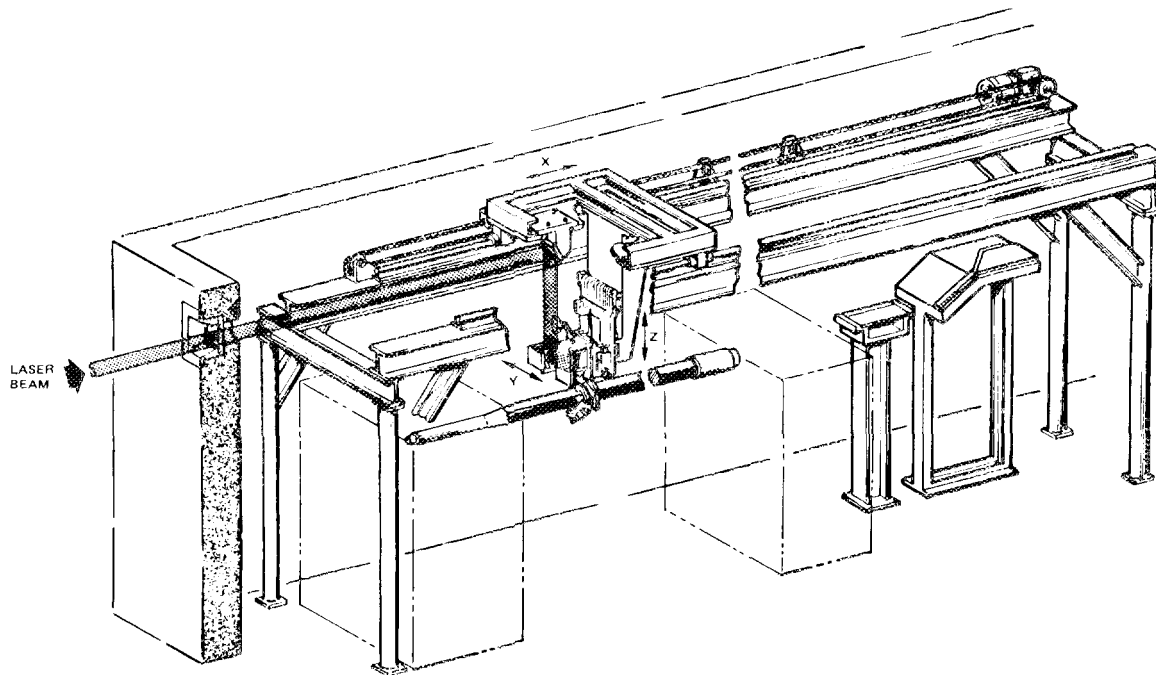


Fig. 6.2. Isometric view of laser cutting system.

6.1.1 Gantry assembly

The support structure for the cutting system utilizes steel I-beams in its construction. As shown in Fig. 6.1, these I-beams form an open-box framework which straddles the fuel subassembly and its rotating mechanisms. The dimensions indicated in Fig. 6.1 are subject to change, depending on the design constraints imposed by the fuel subassembly rotating and handling mechanisms.

Along the top of the longitudinal I-beams are mounted precision roundways which support the "X"-motion carriage. The "X" carriage supports and carries the "Z"-turning mirror, focus head, and shroud follower assemblies. The rectangular opening in the top of the "X" carriage allows the laser beam to enter the focus head and vertical removal of the focus head assembly from the system.

The drive system to traverse the "X" carriage over the fuel subassembly could consist of a stepping motor-gearbox combination and either a ball screw or chain drive with support rollers along the chain length, as shown in Fig. 6.2. The control system incorporates a stepping

motor translator, microprocessor, and other related components to control acceleration, velocity, position of the "X" carriage (i.e., longitudinal beam location), and other sequential control functions.

The "Z" mirror, as mentioned earlier, is mounted on the top of the "X" carriage and directs the horizontal incoming laser beam down into the focus head assembly. The "Z" mirror, as well as the mirrors in the focus head assembly, are solid copper with gold-coated reflective surfaces. As shown in the analysis section, water-cooling is not required for these mirrors. Adjustment screws on the top surface of the "Z" mirror mount permit remote alignment of the mirror to aim the laser beam into the focus head. Removal of the "Z" mirror is accomplished by loosening a captive bolt and lifting the assembly vertically from two locating pins.

At the extreme right of the support structure is a rest station for the "Z" carriage. Loading and unloading of the fuel subassemblies and removal and replacement of system components take place with the "X" carriage in this rest location. Also, the rest station provides a known position for the "X" carriage and focus head motions, allowing a repeatable starting point for any cutting sequence. As the "X" carriage is driven toward the rest station, a roller on the bottom of the focus head contacts a vertically-inclined surface which pushes the focus head "Z" motion to its extreme vertical position. Continued travel by the "X" carriage causes the focus head to contact a horizontally-angled surface which pushes the "Y" motion to its extreme left position.

6.1.2 Focus head assembly

The focus head assembly attaches to the "X" carriage and incorporates three mirrors to direct and focus the laser beam onto the shroud surface. The annular characteristic of the unfocused laser beam allows on-axis focusing, using a spherical focusing mirror (see Fig. 4.3). Pertinent design features are shown in Fig. 6.3, and an isometric sketch is shown in Fig. 6.4.

As the unfocused beam enters the focus head, it is turned horizontally by a "Y"-motion flat-turning mirror. The beam then strikes an

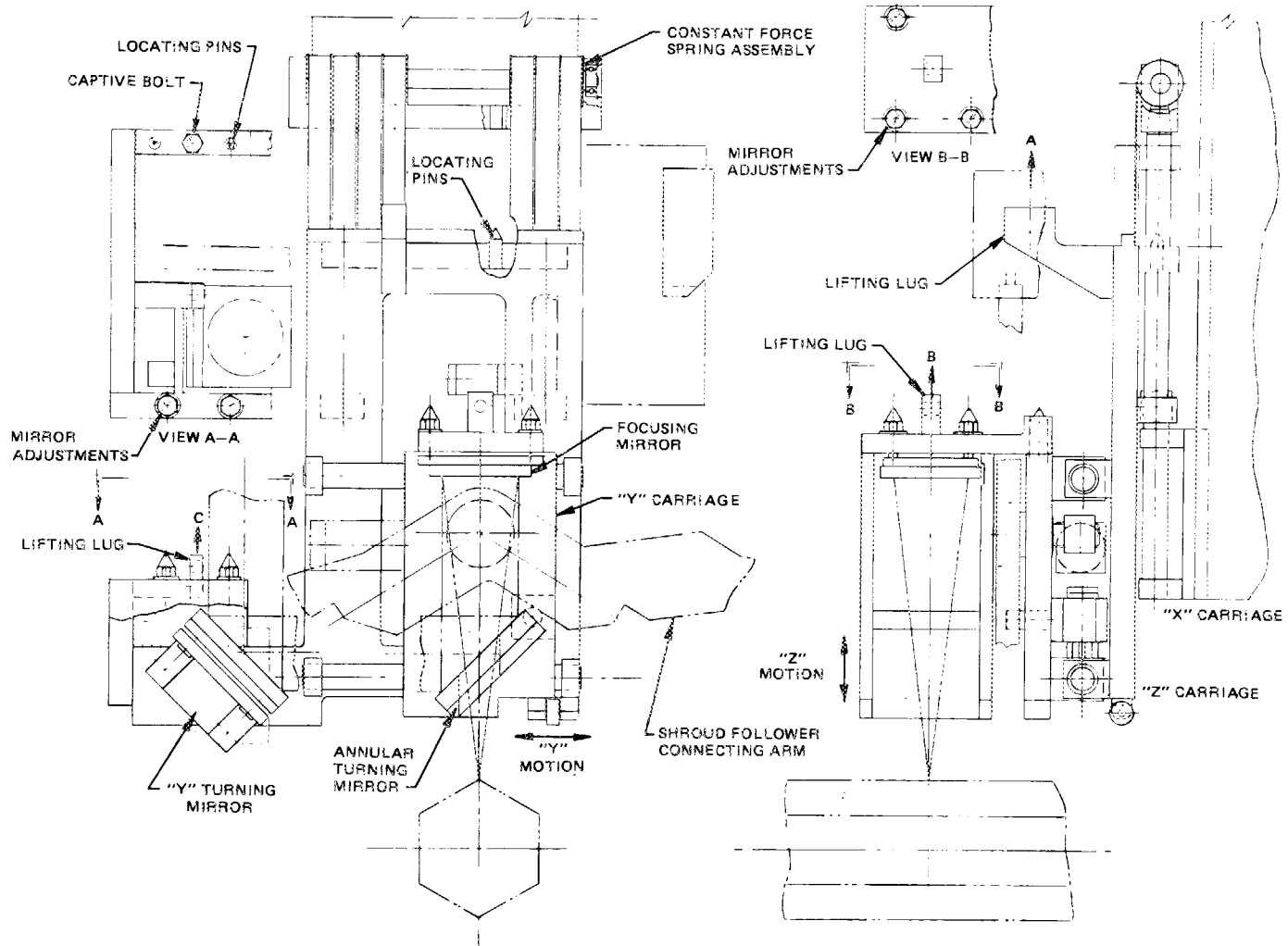


Fig. 6.3. Focus head assembly.

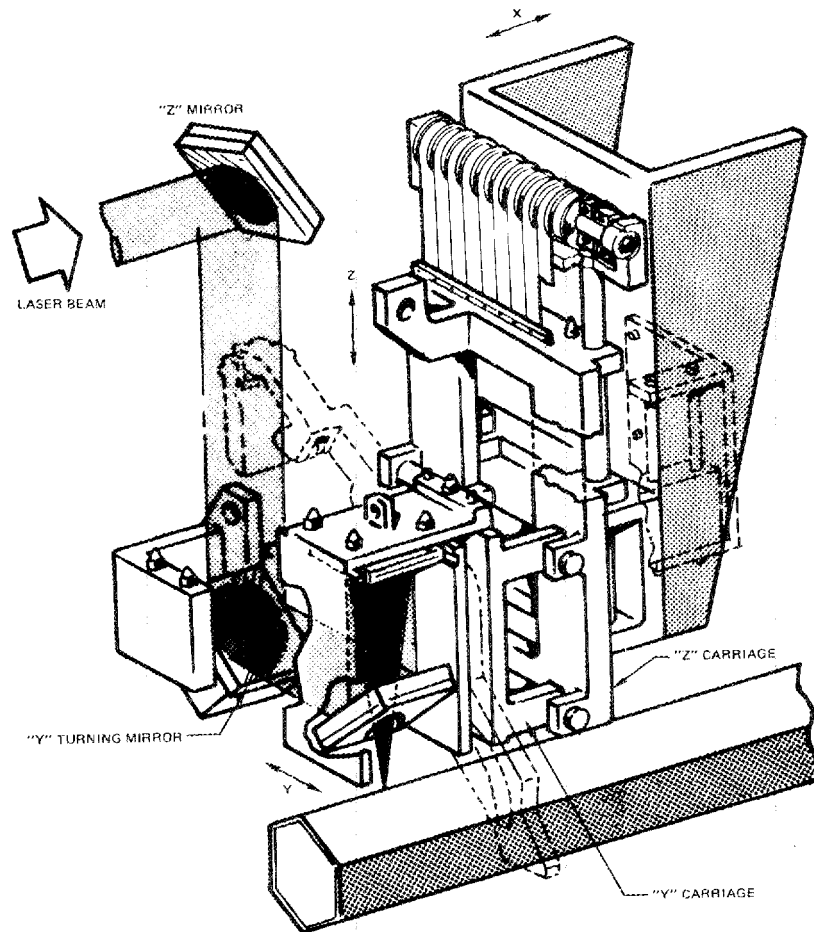


Fig. 6.4. Isometric view of focus head assembly.

annular flat-turning mirror, directing the beam upward onto the spherical focusing mirror. The focusing mirror, with a nominal focal length of 30 cm, is positioned to direct the beam through the opening in the annular-turning mirror onto the shroud surface.

To keep the beam focal point positioned properly on the shroud surface within the expected fuel subassembly tolerances of a two-degree twist and a 10-cm maximum bow, a mechanical shroud follower (described in the next section) is employed which moves the focus head mirrors in vertical "Z" and horizontal "Y" directions. A pneumatic actuator rotates the circumferential or the longitudinal shroud follower into position.

A "Z"-motion carriage supports the entire focus head assembly. The "Z" carriage attaches to the "X"-motion carriage on the support structure. Vertically-oriented, precision, low-friction hardened roundways and ball-bushings provide ± 10 cm of the "Z" (vertical) motion. To minimize the downward gravity force of the focus head (approximately 90 kg) as the mechanical follower is traversing the fuel subassembly, a series of constant force springs is attached between the top of the "Z" roundways and the top of the "Z" carriage. These springs effectively perform the same function as a counterweight.

A nominal ± 10 cm of horizontal motion is achieved through a "Y"-motion carriage supported by the "Z" carriage. The annular turning mirror and the spherical focusing mirror are mounted on the "Y" carriage, which is free to move laterally on horizontal hardened roundways and ball-bushings. The "Y"-turning mirror is mounted to the "Z" carriage and aligned in such a manner that during "Y" and "Z" motions, the laser beam is always positioned correctly on the annular turning mirror. Pneumatic actuators lock "Y" and "Z" motions as required during system operation.

Alignment of the "Y"-turning mirror and the spherical focusing mirror is accomplished by turning the adjustment screws on the top surface of the mounts (Fig. 6.3, views A-A and B-B). The annular-turning mirror is fixed and is aligned at initial assembly.

The focus head is designed for long life; however, maintenance and replacement of optical components will be necessary at periodic intervals. Provision has been made in the design for total or partial disassembly and removal from the system. The entire focus head assembly is removed by lifting vertically at the lifting lug that is mounted on the top of the "Z" carriage (Fig. 6.3, point A). As the "Z" carriage is raised, locating pins on the top of the carriage engage holes in the cross support yoke of the constant force spring assembly. Continued lifting pulls the spring assembly and "Z" carriage from the ends of the roundways; the entire focus head assembly is disengaged from the system. The "Z" roundways remain permanently attached to the "X" carriage. The ends of the "Z" roundways are tapered to guide the ball-bushings during the reassembly and reattachment of the spring assembly.

The focusing mirror and the annular-turning mirror are removed as a unit by loosening a captive bolt and lifting the assembly vertically with the lifting lug from two locating pins (Fig. 6.3, B). The procedure is reversed for reassembly. The "Y"-turning mirror can also be removed as a separate unit using a similar procedure (Fig. 6.3, point C).

6.1.3 Shroud follower assembly

The shroud follower consists of two mechanical tracking assemblies designed to move the focus head in appropriate "Y" and "Z" motions to maintain the focal point of the laser beam at the correct location during cutting. One assembly follows the contour of the fuel subassembly shroud during circumferential cutting, and the other assembly follows the shroud contour during longitudinal cutting. Both follower assemblies incorporate the necessary assist-gas jets for effective cutting. These assemblies are shown in Figs. 6.5 and 6.6. Figure 6.7 is an isometric sketch. The follower assemblies are tied together through a common connecting arm, which, in turn, is attached to the "Y" carriage at a rotary pivot point (Fig. 6.5, point A). All movement resulting from the forces exerted on the follower assemblies during tracking is transmitted to the focus head at this pivot point. Rotation of the connecting arm by a pneumatic rotary actuator brings either follower assembly into position. A pneumatic lock holds the follower assembly in a horizontal neutral position when desired.

The circumferential follower is attached to the left end of the connecting arm and has two rollers which contact the top and left side surface of the shroud when brought into position. A horizontal locating guide is attached and pivots at the side roller. Mounted to the "X" carriage is a sliding weight; its function is explained in the following operating description.

Prior to operation, the following initial conditions apply: (a) the "X" carriage is in the rest station; (b) the follower connecting arm is in the neutral position and locked; (c) "Y" and "Z" focus head motions are locked; (d) the fuel subassembly is locked in place with one corner oriented straight up (as shown in Fig. 6.5).

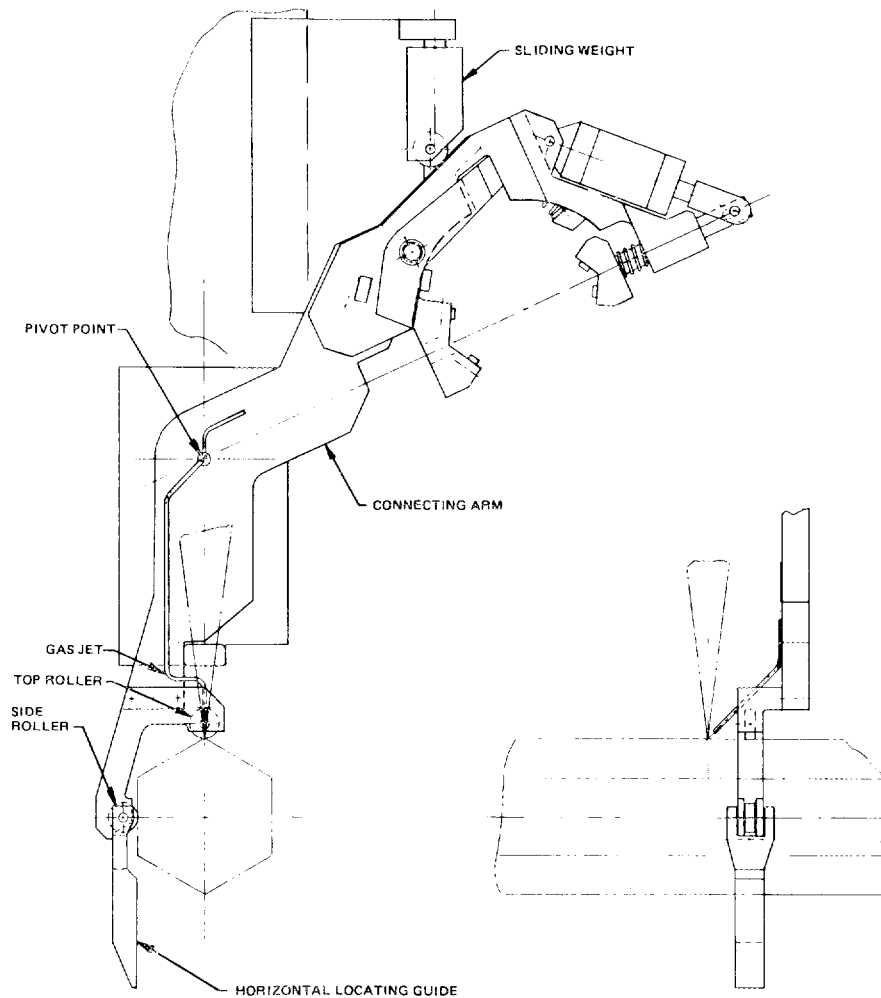


Fig. 6.5. Circumferential shroud follower.

The "X" carriage moves into position to make the initial circumferential cut. The connecting arm is unlocked and rotated counterclockwise until it contacts a mechanical stop on the "Y" carriage. The rotary pneumatic actuator remains energized during the circumferential cut cycle. At the same time, an inclined plane surface on the right side of the connecting arm lifts the sliding weight vertically (see Fig. 6.5). The "Y"-motion pneumatic lock is released and the "Y" carriage is driven to the right by the gravity force of a sliding weight (mounted from the "X" carriage and free to slide only in the vertical direction) pushing on the 45°-inclined surface. The "Y" motion continues until either the

ORNL DWG. 78-19453

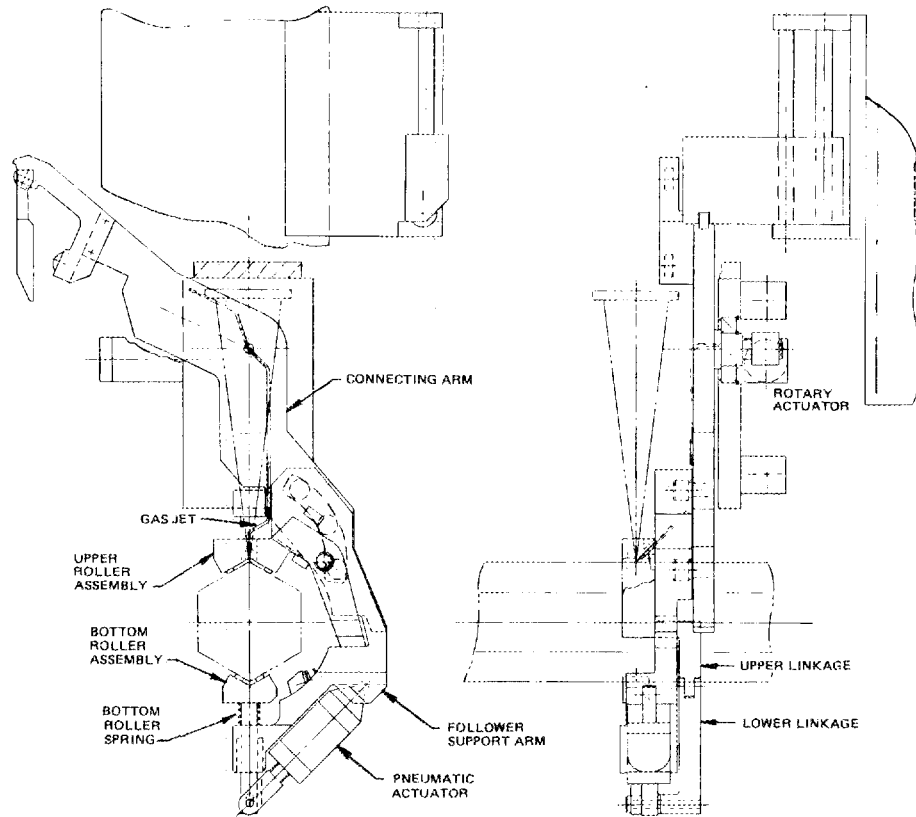


Fig. 6.6. Longitudinal shroud follower.

ORNL DWG. 78-19457

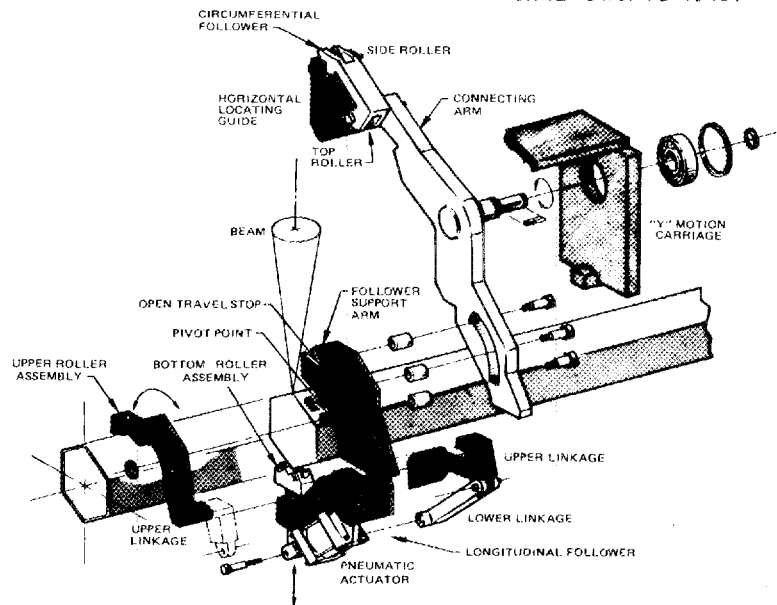


Fig. 6.7. Exploded view of shroud follower assembly.

horizontal locating guide or the side roller contacts the left flat surface of the shroud. Once contact has been made, the "Z"-motion pneumatic lock is released, and the sliding weight drives the focus head vertically until the top roller impacts the top hex point on the shroud. The circumferential cut is now made by turning on the laser and gas jet and rotating the fuel subassembly 360°. The side and top rollers are kept in contact with the shroud surface during rotation by the sliding weight. After completion of the circumferential cut, the "Y" and "Z" focus head motions are locked to maintain the location of the beam impingement point.

The longitudinal follower (Fig. 6.6) is attached to the right end of the connecting arm and consists of top and bottom roller assemblies mechanically tied together. Both of the roller assemblies have two rollers positioned to follow the shroud surface on either side of the hex points. The roller assemblies are tied together by lower and upper linkages.

The bottom roller assembly is spring-loaded and is connected to a pneumatic actuator rod and the lower linkage. The connection point is slotted to allow vertical motion of the bottom roller assembly to compensate for changes in the shroud width during longitudinal cutting.

To open the roller assemblies for initial positioning and removal, the pneumatic actuator is energized. This results in a downward force on the bottom roller assembly. At the same time, the lower linkage pulls on the bottom of the upper linkage, causing it to rotate about its pivot point (see Figs. 6.6 and 6.7) and raising the upper roller assembly. The open travel is limited by the upper linkage coming in contact with the open travel stop. To close the roller assemblies for contact with the shroud surface, the pneumatic actuator is deenergized and the forces exerted by the bottom roller spring and the upper linkage spring bring the roller assemblies into position.

To maintain beam position during cutting as the shroud surface twists, the roller assemblies follow the surface change through the mechanical connection between the follower support arm and the connecting arm. This mechanical connection was designed to allow angular movement between the follower support arm and the connecting arm. Three rollers

ride in a slot in the connecting arm (Fig. 6.7) and are positioned such that they follow a center of rotation about the beam impingement point on the fuel subassembly shroud. An angular change in the follower support arm results in a force on the connecting arm which is translated into appropriate "Y" and "Z" focus head motions through the connecting arm pivot point.

6.1.4 Calibration station

The calibration station shown in Fig. 6.1 is an area where laser cuts on test samples can be made to determine if all cutting parameters are correct before proceeding with the fuel subassembly cutting. Performing the calibration cut prior to cutting each fuel subassembly allows compensation of power, speed, or alignment for hourly or daily changes in cutting capability due to mirror absorption changes, laser mode changes, or other factors. The test sample support structure has one open side to allow possible viewing of the underside of the calibration sample with a TV system.

When the test sample is in place, the sample top and rear vertical support walls are in the same spatial relationship as the top hex point and the left flat wall on the shroud. This relationship allows the circumferential follower to determine the beam impingement point once the focus head is brought into position over the test sample. After the sample cut is made, the focus head is driven back to the rest station prior to beginning fuel subassembly cutting.

6.1.5 Typical cutting sequence

The following is a typical cutting sequence of a fuel subassembly. Initially, the following conditions apply: (a) the focus head is at the rest station, (b) the "Y" and "Z" focus head motions are locked, (c) the shroud follower is in the neutral position and locked, and (d) a test sample is in place. Left and right are defined from the vantage point given by a view of the system as in Fig. 6.2 or the side view of Fig. 6.1.

For a sample cut, the focus head is driven to the left until positioned over the left side of the test sample. The shroud follower

is unlocked and the circumferential cutting assembly is swung into position to determine the beam impingement point. The focus head is driven to the right, and a sample cut is made. The follower assembly is returned to the neutral position and locked. The focus head is driven to the right, onto the rest station, establishing "Y" and "Z" initial positions. Then the "Y" and "Z" positions are locked, while inspection of the sample proceeds. At this time, adjustments can be made to laser power, traverse speed, or mirror alignments, and other sample cuts can be made until a test cut is judged satisfactory.

To make the left circumferential cut, the focus head is driven to the left until positioned over the lower circumferential cut area of the fuel subassembly, and the circumferential follower is swung into position. With the laser on, the fuel subassembly is rotated 360° , the laser cut is made, and the laser is turned off. The "Y" and "Z" focus head motions are locked to complete the cut.

To make the longitudinal cut, the longitudinal follower is swung into position, the laser is turned on, the focus head is driven to the right, and the laser cut is made. After the laser is turned off, the "Y" and "Z" motions are locked to complete the cut.

The final right circumferential cut is accomplished by repeating the left sequence; however, the total process is complete when the focus head is returned to the rest station.

6.1.6 System features to be designed

There are two features of the laser cutting system which do not appear on the drawings (Figs. 6.1 through 6.7) but would have to be incorporated into the system. Needed features are (1) a reflective heat shield around the focus head to reduce the heat load from the hot fuel subassembly, and (2) some form of purge box around the mirrors in the hot cell to prevent dust from settling on the mirror surfaces.

6.2 System Specification

Based on the tests, analysis, and design work reported above, the following preliminary system specification is given for a laser disassembly system to function in a hot-cell environment.

6.2.1 Laser system and optical train

The following specifications define the requirements for the laser source and laser beam transmission to the focus head.

- a. Laser type — CO₂, cw, and electric discharge, to be placed outside the cell.
- b. Laser rated power level — 3 kW, continuous, $\pm 2\%$ short-term (1 h) stability, and $\pm 5\%$ long-term stability.
- c. Beam size and type — 5- to 8-cm diam, unstable oscillator with beam magnification ≥ 1.8 .
- d. Hot-cell laser window — Solid (NaCl, KCl, or ZnSe). Requires further study.
- e. In-cell mirrors — Uncooled solid copper slabs and front surface gold-coated.
- f. Optical train — Four mirrors, to turn and focus beam. Mirrors to be enclosed by purge boxes (to be designed).
- g. Mirror installation — Means required for adjusting, removing, and replacing individual mirrors.
- h. Power control — Laser power must be controlled to provide continuous cutting through the raised load pad on the fuel subassembly.

6.2.2 Focus head features

The following specifications define the required features of a remotely operated laser focus head.

- a. F/number: 4 to 6.
- b. Assist-gas jet — Ambient cell gas, 345 kPa, and nonclogging design, required for both circumferential and longitudinal cuts.
- c. Focus head cutting speed — 50 to 128 cpm, infinitely variable.
- d. Focus head control — Preferably, ball screw drive along fuel subassembly axis, mechanical follower to provide capability of following fuel shroud surface through ± 10 cm bow and 2° twist. Focal point to be maintained on shroud surface to ± 0.6 -mm-vertical variation and ± 1.2 -mm variation in horizontal plane.

- e. Radiation resistance — Focus head parts to resist radiation levels of $5 \cdot 10^6$ rd/h for thousands of hours.
- f. Temperature control — Focus head must be designed to work on fuel subassemblies with surface temperatures in the range of 260 to 540°C.

6.2.3 Mechanical

The following specifications define the required mechanical features of the general laser system.

- a. Cutting gantry — Must be able to straddle fuel assembly to allow easy loading of assembly.
- b. Modularity — Entire focus head and moving carriage must be removable and replaceable.
- c. Optics — All mirrors must be remotely adjustable, as well as removable and replaceable.
- d. System calibration — Means must be provided for regular monitoring of system cutting capability, and adjusting same by adjusting laser power, speed, or aligning mirror train.
- e. Environmental control — To ease gas makeup requirements in hot cell, cutting gas and beam tube purge gas should be taken from cell environment.

7. CONCLUSIONS

1. Nuclear fuel subassembly shrouds can be cut apart by a laser with very little risk of perforating the cladding of adjacent fuel rods if the cut is made in a corner of the hexagonal shroud containing a solid dummy pin. A hollow dummy pin with the same wall thickness as the fuel pin could also be used to shield fuel rods, but the tolerance to variations would not be as great.
2. Fuel rods spaced away from the shroud wall by a 1.4-mm wire allow cutting of the shroud without puncturing the underlying fuel cladding if laser power and cutting speed are in the range of 1.5 to 2 kW and 65 to 77 cpm respectively. It is estimated that power and speed

would have to be maintained within $\pm 5\%$, and that work distance (i.e., focusing mirror to workpieces surface) could not vary more than ± 0.5 mm, assuming the use of a focusing system with an f/number of approximately 5. These conclusions are based on the use of an air jet. Use of nitrogen gas with 5% oxygen would increase the power requirements somewhat.

3. If the fuel rod is close to (< 0.5 mm) or in contact with the shroud, the shroud cannot be cut without puncturing the fuel cladding.
4. The best way to cut the shroud is to orient the beam normal to its surface such that the wall thickness to be cut is minimized. Off-normal orientation, which effectively increases the thickness to be cut, results in more risk of damage to underlying fuel pin walls.
5. A jet-assist nozzle with a minimum flow diameter of 3 mm, which can be located approximately 11 mm from the laser beam interaction point, is effective in material removal and is not overly subject to fouling during cutting.
6. Minimum penetration into underlying fuel cladding can be obtained by orienting the jet-assist axis at a small angle ($\sim 30^\circ$) to the shroud surface.
7. Argon gas in the space between the fuel rod and the shroud is a deterrent to penetration of the cladding.
8. Air, nitrogen, or carbon dioxide jet-assist gases result in satisfactory cutting of the shroud material, however, oxygen-rich mixtures greater than 50% cause more extensive damage to underlying fuel rods.
9. Small f/number focusing systems (between f/4 and f/6) provide the least risk of puncturing the fuel cladding when cutting the shroud.
10. Of the five different approaches for guiding the focus head along the fuel shroud as defined in this study, a passive system in which the focus head is guided directly by the fuel subassembly is the most desirable in terms of simplicity, reliability, lack of data storing or processing, and low cost. The major drawback of this system is that it may put significant force on the fuel subassembly.
11. If the loads imposed on the fuel subassembly by the completely passive focus head steering system are too great, and alternate method incorporating a power boost between the fuel subassembly

follower and the focus head can be used. This power boost would be activated by error signals generated by the differences in position between the focus head and the fuel shroud follower, and thus, would not require any special data storage or handling.

12. Of the various fuel followers considered, a simple wheeled yoke with rollers that roll directly on the shroud surface appears to be the simplest, most reliable design approach.
13. Inside the hot cell, optical elements used to transfer and focus the laser beam should be front surface reflective mirrors rather than transmissive elements. For the duty cycles (5 min maximum per half hour) and power levels (3 kW max) foreseen for the fuel disassembly task, these mirrors do not need to be water-cooled.
14. Heat radiation shielding will probably be required around the focus head to shield it from the high temperature of the fuel subassembly.
15. To monitor small changes in the laser system cutting capability, a calibration station where a sample cut could be made and examined periodically may be required. This technique would give warning of changed cutting conditions due to mirror degradation, optical train misalignment, beam mode or power changes, or any other circumstance that could alter the system's cutting capability.
16. On the hot cell heat loads due to laser cutting are negligibly small relative to the heat released from the fuel subassembly itself.
17. The laser appears to offer basic advantages for disassembling nuclear fuel elements in its ability to cut by remote control with minimum dross from the cut area and minimum volatilization or other loss of fissionable material. With some limitations, there do not appear to be any basic technical factors prohibiting the use of laser for irradiated reactor subassemblies.

8. RECOMMENDATIONS

Additional cutting tests are recommended. These tests should involve the use of a single fuel rod and shroud configuration. The tests should consider the use of power ramping to cut the load pad region of the fuel subassembly, the minimum spacing between rod cladding and shroud that will allow laser cutting without breaching the cladding,

a detailed assessment of the fissionable material that could be released in the event of rod cladding damage, and tests which evaluate circumferential cutting.

A critical element in establishing the feasibility of the disassembly device proposed in this study is the operation of the mechanically driven focus head and follower. It is therefore recommended that a follow-on study provide for the design, fabrication, and test of a focus head and follower to firmly establish the feasibility of this approach.

As a final recommendation, there should be, in the future, closer interaction between reactor fuel designers and fuel reprocessors to develop future reactor fuel subassemblies that have disassembly features without compromising neutron economy and breeding gain.

ACKNOWLEDGMENT

The authors would like to acknowledge those at United Technologies Research Center who were responsible for performance of the technical work reported herein. These men and their areas of study were:

Raymond F. Duhamel -- Laser Cutting Tests

Allan P. Walch -- Laser Focus Head Control and Sensors

Paul R. Blaszk -- Optical Components Analysis and Heat and Mass
Flow Additions to Cell

Warren C. Ball -- System Design and Cost Estimation

Antonio B. Caruolo -- Mechanical Design

REFERENCES

1. A. Mills, United Kingdom Atomic Energy Authority, private communication, June 1978.
2. R. Masters, *Nucl. Eng. Int.*, 21, 249 (1976) p. 42.
3. I. J. Spalding, "Applications of High-Power Lasers," in proceedings of the *International Symposium on Gasdynamic and Chemical Lasers*, October 11-15, 1976, Koln-Oors, Germany, p. 499-519.

4. J. Martin and J. Bernard, "Application of a Laser Beam to Fuel Element Decladding," paper presented at the *NUCLEX 72 International Nuclear Industries Fairm October 16 to 21, 1972, Basel, Switzerland* (translated from French by STS Incorporated under Order 16091 from Argonne National Laboratory).
5. James E. Murray, "Laser Applications Feasibility Study," report by Holobeam, Incorporated to Argonne National Laboratory under contract No. IF-28524, no date (1972 document referred to in report).
6. Denis Yeo, "Nuclear Reactor Fuel Element Splitter," U.S. Patent 4,000,391, December 28, 1976.
7. B. S. Weil, A Request for Proposal to Perform a Conceptual Study for a Laser Disassembly Development Unit, Union Carbide Corporation, Nuclear Division, Attachment C, P.O. #73X56956V, August 4, 1977.
8. M. J. Rennich, ed., "Guidelines for the Design of Remotely Maintainable Equipment," prepared by the Oak Ridge National Laboratory Experimental Engineering Staff, December 1977.
9. A. H. Wilson, "Theory of Metals," Second edition, Cambridge University Press (1953).
10. V. V. Chechetenko et al., "Study of the Effect of Proton Bombardment on the Optical Constants of Thin Metallic Films," *Opt. i. Spektrosk.*, 21, 626-30 (1966).
11. E. J. Szetela and A. K. Chalfant, "Thermal Distortion of Mirrors," paper presented at the *North American Thermal Analysis Society Meeting, St. Louis, Missouri*, September 1977.
12. P. R. Blaszk, "Thermal Stress-Induced Failure of Alkali-Halide Windows," United Aircraft Research Laboratories Report UAR-R28, February 1975.
13. W. A. Sibley and E. Sonder, "Hardening of KCl by Electron and Gamma Irradiation," *J. Appl. Phys.* 34, 8, 2366-70 (1963).
14. J. R. Hopkins, "Comparison of Vacancy and Interstitial Hardening in KCl," *Phys. Status Solidi (A)* 18, K15 (1973).
15. J. S. Nadeau, "Hardening of Potassium Chloride by Color Centers," *J. Appl. Phys.* 34, 8, 2248-53 (1963).
16. P. Kraatz and T. ZolTai, "Effects of Ionizing Radiation on Cleavage Surface Energy of SrF₂," *J. Appl. Phys.* 45, 11, 5093-95 (1974).

17. J. S. Nadeau, "Radiation Hardening in Alkali-Halide Crystals," *J. Appl. Phys.* 35, 4, 1248-55 (1964).
18. H. G. Lipson et al., "The Effect of Ionizing Radiation on the 10.6 μm Absorption of KCl and NaCl," *Phys. Status Solidi (A)* 37, 547-52 (1976).
19. T. J. Magee et al., "The Influence of High-Energy Electron Irradiation on the 10.6 μm Absorption of Mixed KCl Crystals," *Phys. Status Solidi (A)* 30, 81-86 (1975).

INTERNAL DISTRIBUTION

- | | | | |
|--------|-------------------|---------|-------------------------------|
| 1. | S. M. Babcock | 49. | B. E. Lewis |
| 2. | R. E. Benoit | 50. | D. K. Lorenzo |
| 3. | E. D. Blakeman | 51. | A. L. Lotts |
| 4. | R. E. Blanco | 52. | J. L. Marley |
| 5. | J. O. Blomeke | 53. | J. D. McGaugh |
| 6. | R. Blumberg | 54. | L. E. McNeese |
| 7. | B. F. Bottenfield | 55-58. | S. A. Meacham |
| 8. | E. C. Bradley | 59. | J. F. Mincey |
| 9. | N. C. Bradley | 60. | J. G. Morgan |
| 10. | R. E. Brooksbank | 61. | E. L. Nicholson |
| 11. | K. B. Brown | 62. | J. R. Nicholson |
| 12-16. | W. D. Burch | 63. | E. D. North |
| 17. | D. D. Cannon | 64. | W. H. Pechin |
| 18. | J. M. Chandler | 65. | F. L. Peishel |
| 19. | R. M. Counce | 66. | H. Postma |
| 20. | D. J. Crouse | 67-68. | R. H. Powell |
| 21. | J. P. Drago | 69. | J. E. Rushton |
| 22. | B. C. Duggins | 70. | W. F. Schaffer, Jr. |
| 23. | D. E. Dunning | 71. | B. B. Spencer |
| 24. | W. E. Eldridge | 72. | J. G. Stradley |
| 25. | J. H. Evans | 73. | D. W. Swindle |
| 26. | R. E. Eversole | 74. | D. B. Trauger |
| 27. | M. J. Feldman | 75. | W. E. Unger |
| 28. | D. E. Ferguson | 76. | J. E. Van Cleve |
| 29. | J. Garin | 77. | B. L. Vondra |
| 30. | N. R. Grant | 78. | D. C. Watkin |
| 31. | W. S. Groenier | 79-102. | B. S. Weil |
| 32. | M. J. Haire | 103. | T. D. Welch |
| 33. | W. R. Hamel | 104. | G. R. Wetherington |
| 34. | D. C. Hampson | 105. | M. E. Whatley |
| 35. | W. O. Harms | 106. | J. R. White |
| 36. | H. W. Harvey | 107. | R. G. Wymer |
| 37. | J. N. Herndon | 108. | O. O. Yarbro |
| 38. | R. M. Hill | 109. | S. Beard (consultant) |
| 39. | W. D. Holland | 110. | Manson Benedict (consultant) |
| 40. | R. D. Hurt | 111. | L. Burris, Jr. (consultant) |
| 41. | R. A. Jacobus | 112. | A. B. Carson (consultant) |
| 42. | J. D. Jenkins | 113. | G. R. Choppin (consultant) |
| 43. | W. F. Johnson | 114. | E. L. Gaden, Jr. (consultant) |
| 44. | R. T. Jubin | 115. | C. H. Ice (consultant) |
| 45. | A. D. Kelmers | 116. | W. H. Lewis (consultant) |
| 46. | H. T. Kerr | 117. | A. Schneider (consultant) |
| 47. | L. J. King | 118. | L. E. Swabb, Jr. (consultant) |
| 48. | J. Q. Kirkman | 119. | M. J. Szulinski (consultant) |

- | | | | |
|----------|--|----------|--------------------------------------|
| 120. | J. S. Theilacker (consultant) | 126-127. | Laboratory Records |
| 121. | K. D. Timmerhaus (consultant) | 128. | Laboratory Records,
ORNL RC |
| 122. | A. K. Williams (consultant) | 129. | ORNL Patent Office |
| 123-124. | Central Research Library | 130. | Nuclear Safety
Information Center |
| 125. | ORNL — Y-12 Technical Library,
Document Reference Section | | |

EXTERNAL DISTRIBUTION

131. Director, Reactor Division, DOE-ORO
- 132-133. Director, Division of Nuclear Fuel Cycle and Production, DOE,
Washington, D.C. 20545
- 134-135. Director, Division of Reactor Research and Development, DOE,
Washington, D.C. 20545
136. M. L. Bleiberg, Westinghouse Electric Corporation, Advanced
Reactors Division, Waltz Mill Site, P.O. Box 158, Madison,
PA 15663
137. Duane E. Clayton, Battelle Pacific Northwest Laboratory,
P.O. Box 999, Richland, WA 99352
138. Tom Withers, Gulf + Western Advanced Development and Engineering
Center, 101 Chester Road, Swarthmore, PA 19081
139. Jerry M. Friedman, Sandia Laboratories, P.O. Box 5800,
Albuquerque, NM 87115
140. Frank J. Jones, Bechtel Corporation, P.O. Box 3965, San
Francisco, CA 94119
141. Don Bergstadt, Sundstrand Energy System, 4747 Harrison Ave.,
Rockford, IL 61101
142. R. S. Karinen, Programmed and Remote Systems Corporation,
3460 Lexington Ave., St. Paul, MN 55112
143. Robert H. Karlsson, Rockwell International, Atomics International
Division, Rocky Flats Plant, P.O. Box 464, Golden, CO 80401
144. R. E. Mullen, Aerojet Manufacturing Company, 601 South Placentia
Ave., P.O. Box 4210, Fullerton, CA 926342
145. Office of Assistant Manager, Energy Research and Development,
Department of Energy, Oak Ridge Operations Office, Oak Ridge,
TN 37830
- 146-354. Given distribution as shown in TID-4500 under UC-79c, Fuel
Recycle Category (Applied)